MESON 2023, Krakow, Poland, 24. June. 2023

Meson nucleus bound states studied with high-resolution missing-mass spectroscopy

Yoshiki Tanaka (RIKEN)

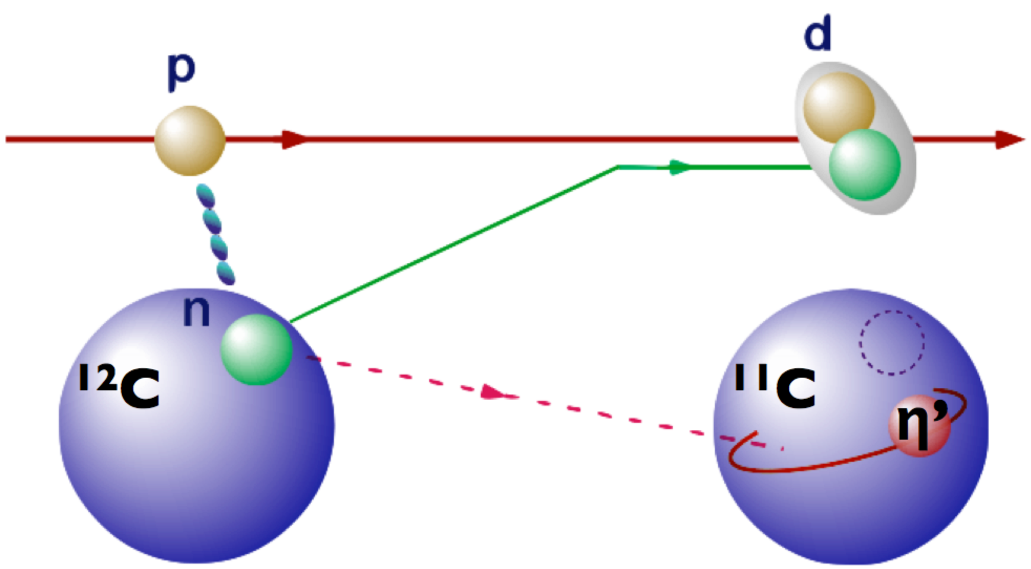

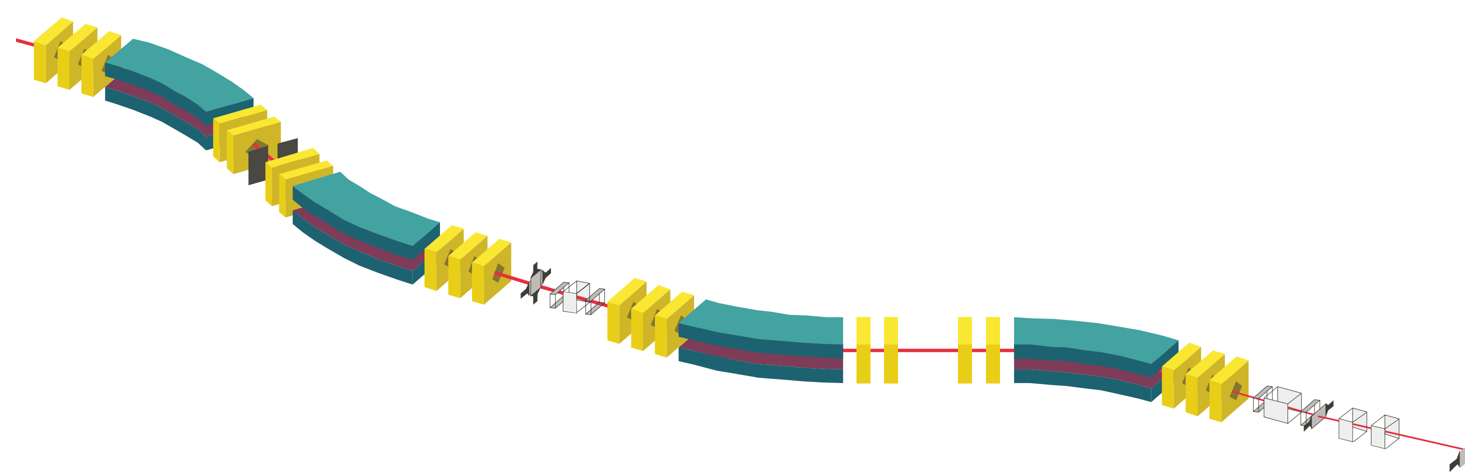

RIKEN GSI PRIME Super-FRS EC MESON 2023

Hadron mass

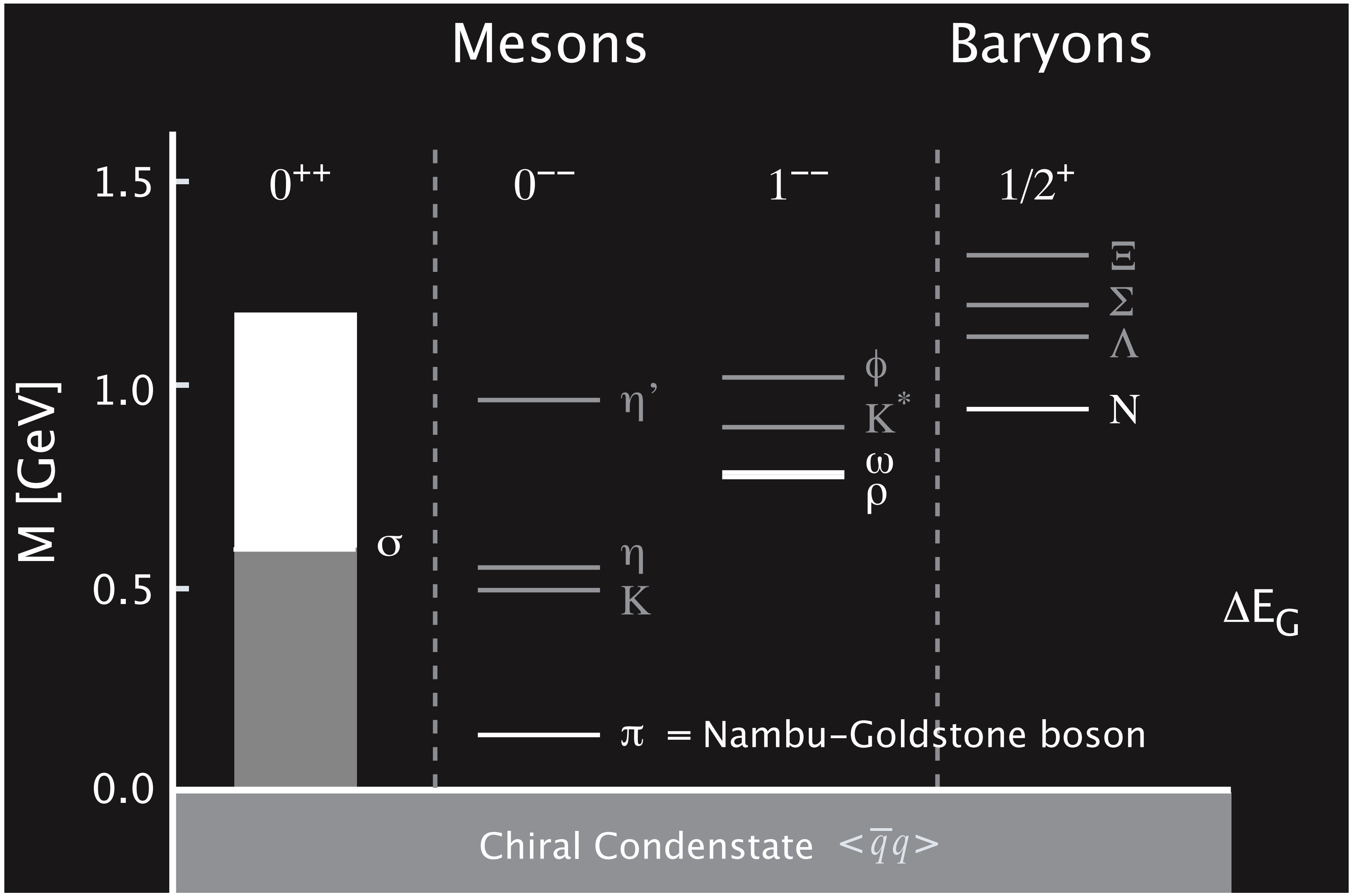

Hayano

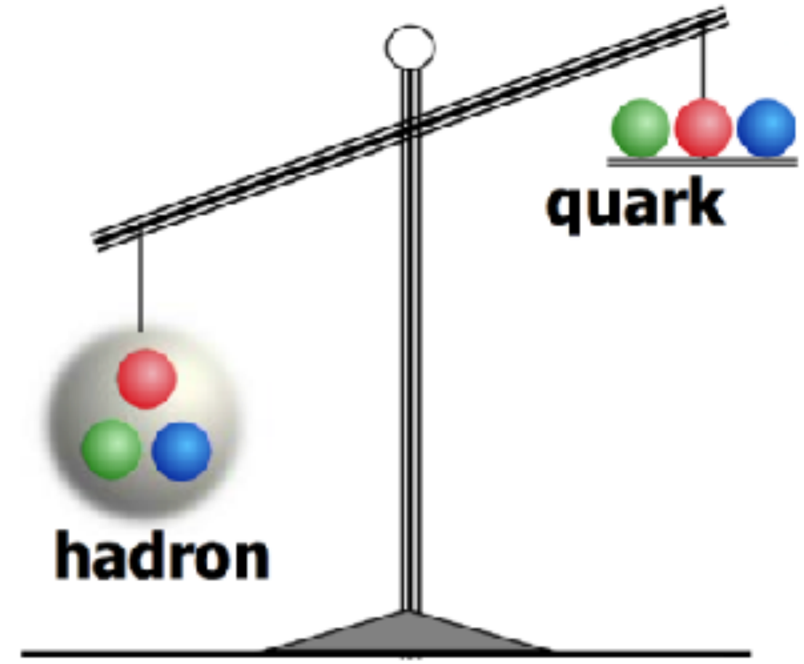

$m_q \simeq$ 3 MeV

$m_N \simeq$ 1000 MeV

"Chiral" condensate

Nambu (1960)

Hatsuda

QCD vacuum : spontaneous breaking of chiral symmetry

- Hadron masses are dynamically generated
- π, K, η ~ Nambu-Goldstone boson

Restoration of chiral symmetry

- Chiral symmetry can be partially restored in finite T and/or ρ
- Hadron properties (e.g., mass, width) under restoration of chiral symmetry

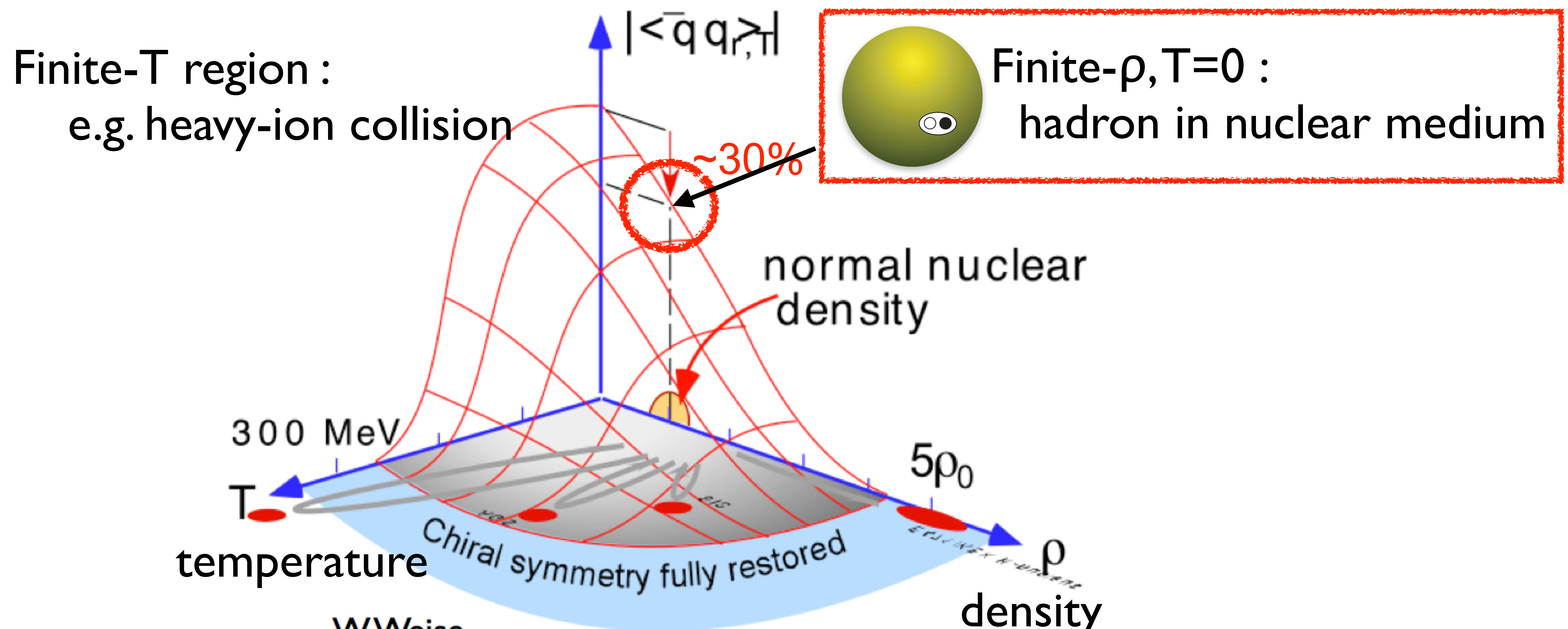

W.Weise, NPA553(93)59.

Experimental approach

Invariant mass spectroscopy

Reconstruct invariant-mass
via e.g. e^+e^- decays

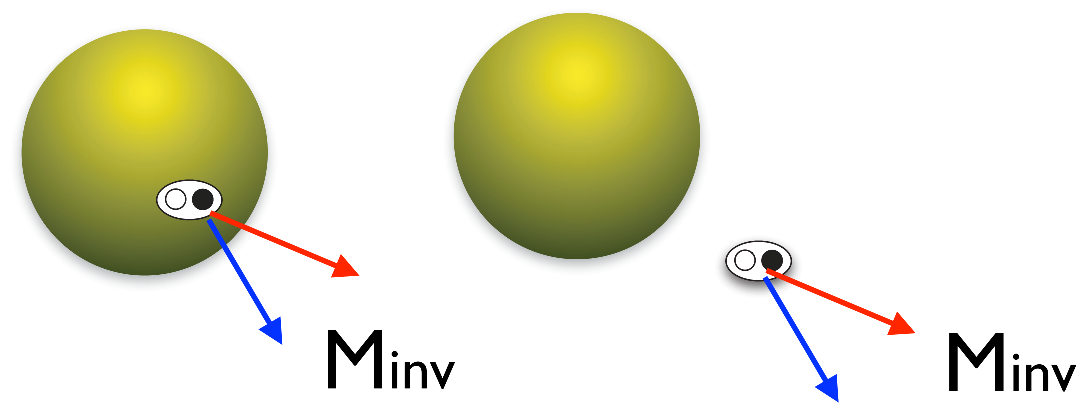

Systematic measurements of meson production

transparency ratio

excitation function

momentum distribution

Spectroscopy of bound states in nuclei

- Well defined quantum states
- Overlap with nucleus → Probe for finite density

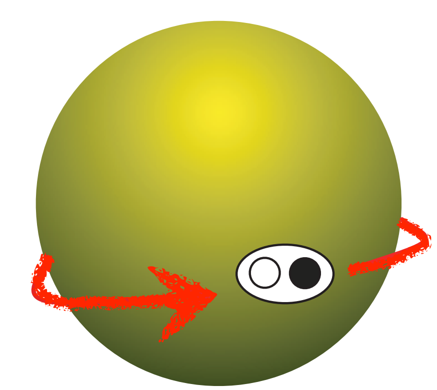

Pseudoscalar mesons

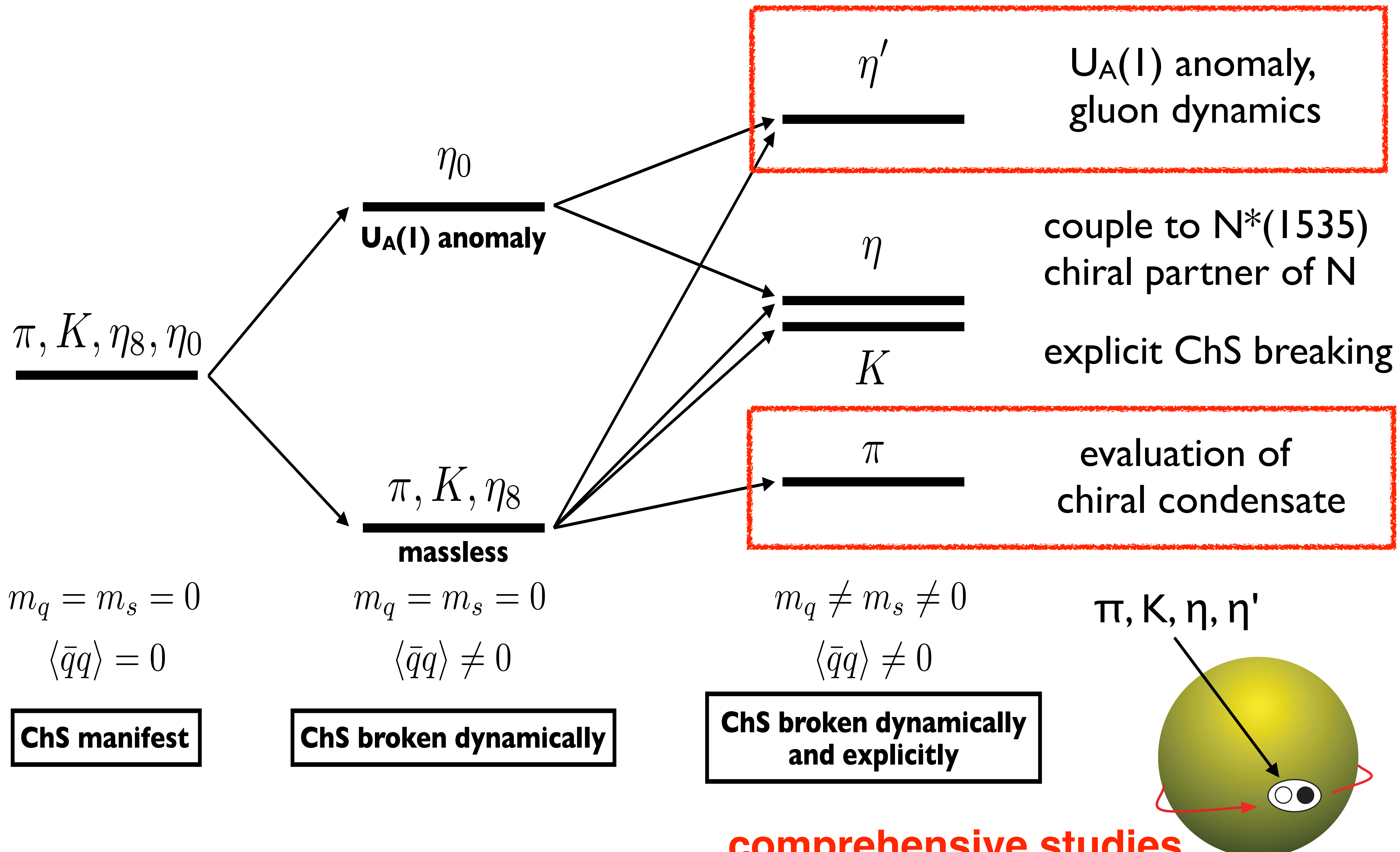

comprehensive studies are important !

H. Nagahiro, D. Jido *et al*, PRC 87, 045201 (2013).
D. Jido, H. Nagahiro, S. Hirenzaki, PRC 85, 032201 (2012).

Spectroscopy of deeply-bound pionic atoms

recent results: **Takahiro Nishi, Kenta Itahashi, et al.,**

nature physics

piAF collaboration, published March 2023

Article

https://doi.org/10.1038/s41567-023-02001-x

Chiral symmetry restoration at high matter density observed in pionic atoms

recent review:

Itahashi, K. (2023). Pionic Atoms in Experiment.
In: Tanihata, I., Toki, H., Kajino, T. (eds) Handbook of Nuclear Physics .
Springer, Singapore. https://doi.org/10.1007/978-981-15-8818-1_36-1

Deeply bound π^- atom

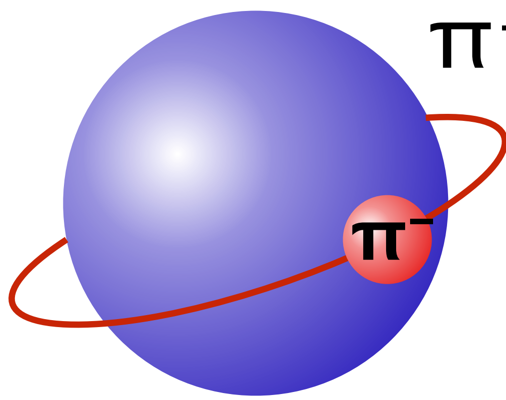

heavy nuclei (Pb, Sn, ...)

Coulomb interaction + strong interaction

deeply bound states (1s, 2p, ...)
near nuclear surface

probe for QCD
in finite density

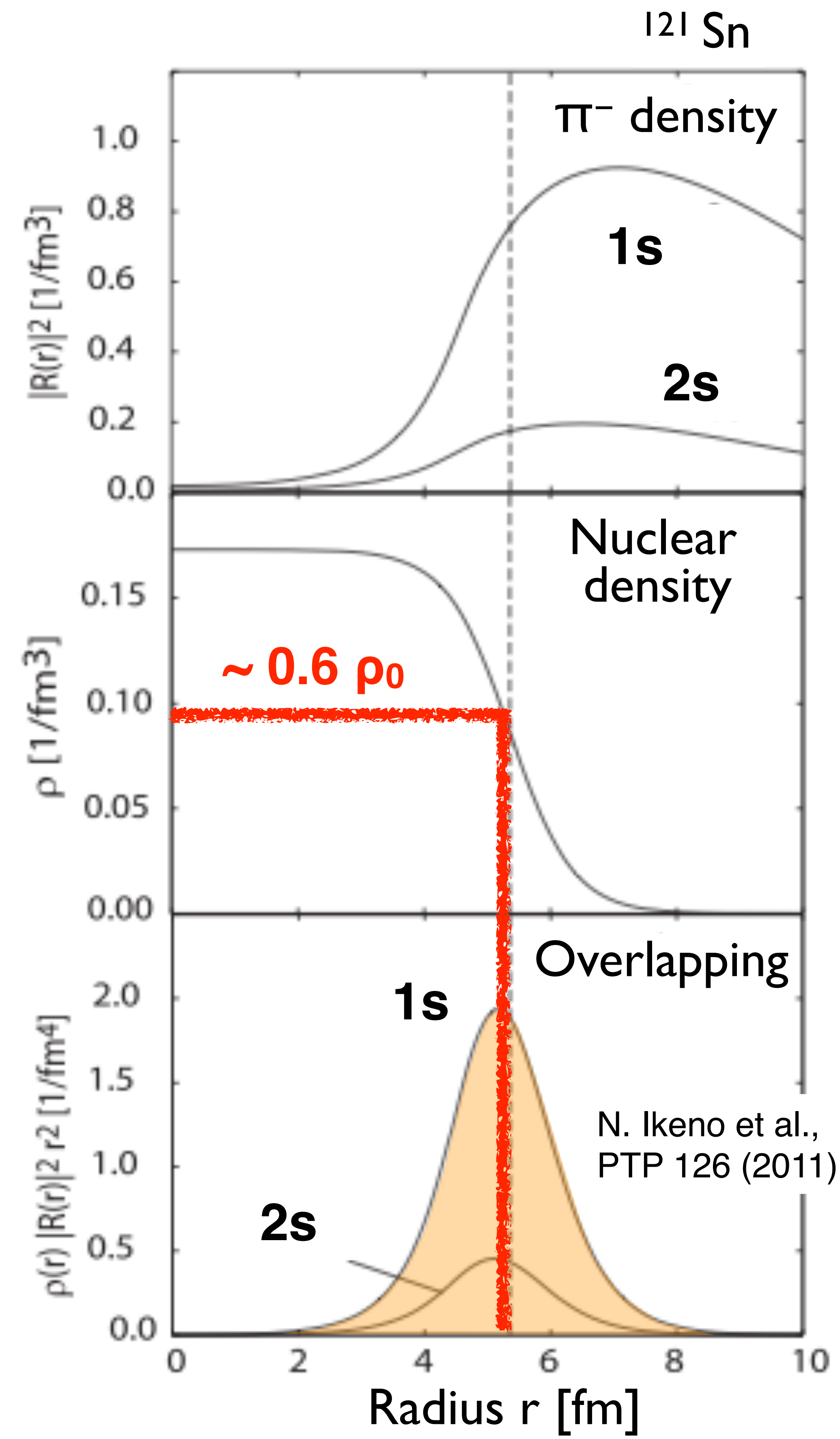

N. Ikeno et al.,
PTP 126 (2011) 483.

Pioneering experiments at GSI

- Discovery with (d, ^{3}He) reaction

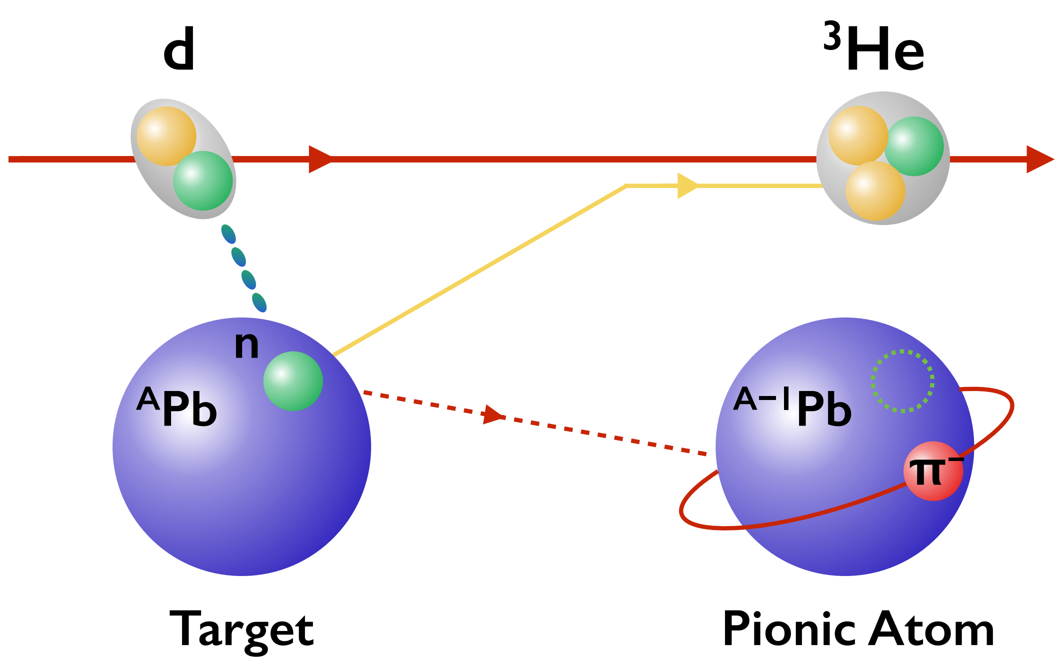

recoil-free kinematics for direct production of deeply-bound states

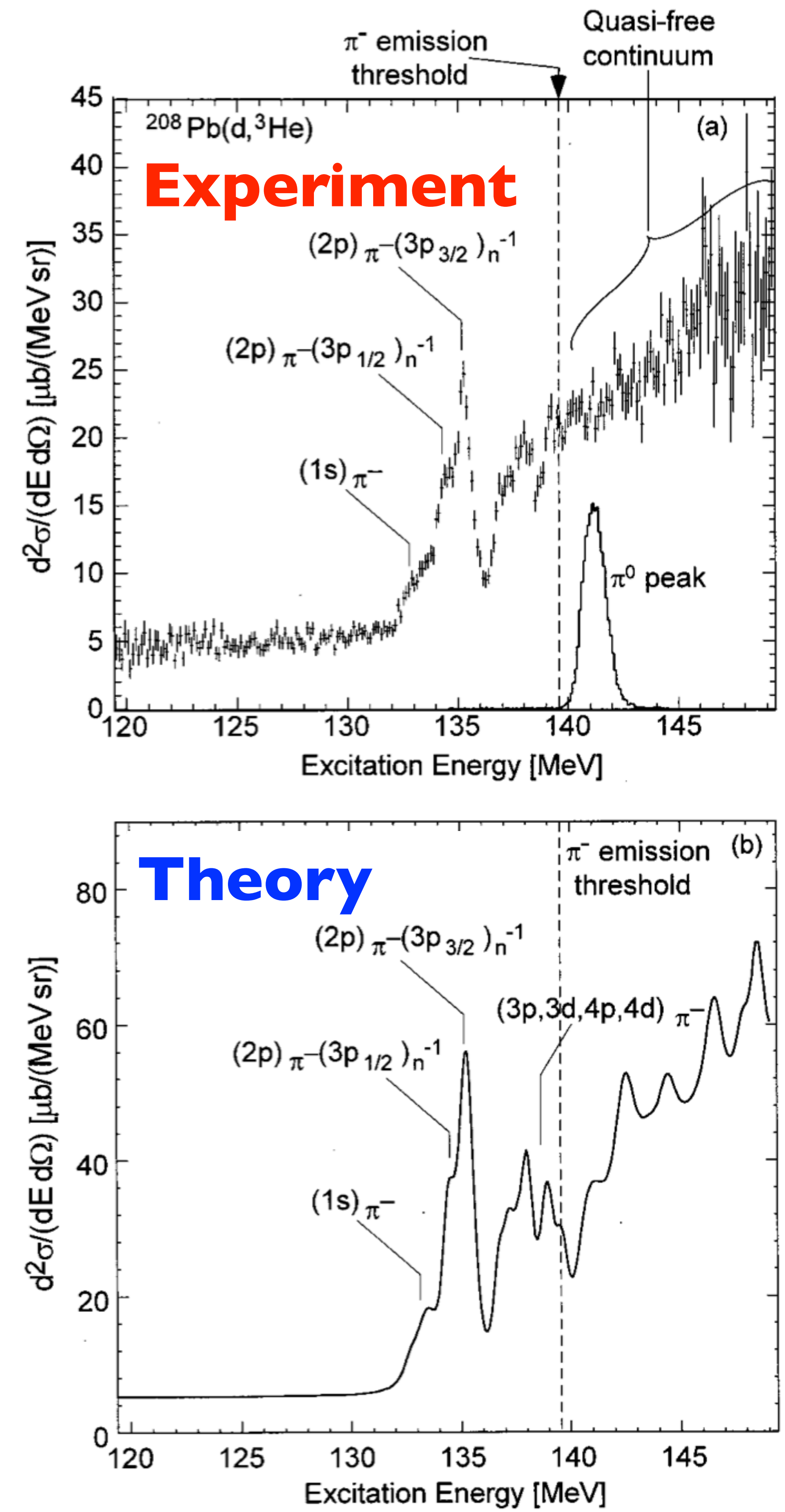

K. Itahashi *et al.*, PRC 62, 025202 (2000)

Itahashi, K. (2023). Pionic Atoms in Experiment.
In: Tanihata, I., Toki, H., Kajino, T. (eds) Handbook of Nuclear Physics .
Springer, Singapore. https://doi.org/10.1007/978-981-15-8818-1_36-1

Pioneering experiments at GSI

- Pionic atoms with Sn isotopes
  - 1s states in $^{115, 119, 123}$Sn observed
  - in-medium s-wave isovector scattering amplitude

$$V_s(r) = -\frac{2\pi}{\mu}[\epsilon_1\{b_0\rho(r) + \underline{b_1\delta\rho(r)}\} + \epsilon_2 B_0\rho(r)^2]$$

  - comparison with free b_1

$$\rightarrow \langle\bar{q}q\rangle_{\rho_0}/\langle\bar{q}q\rangle_0 \approx 0.67$$

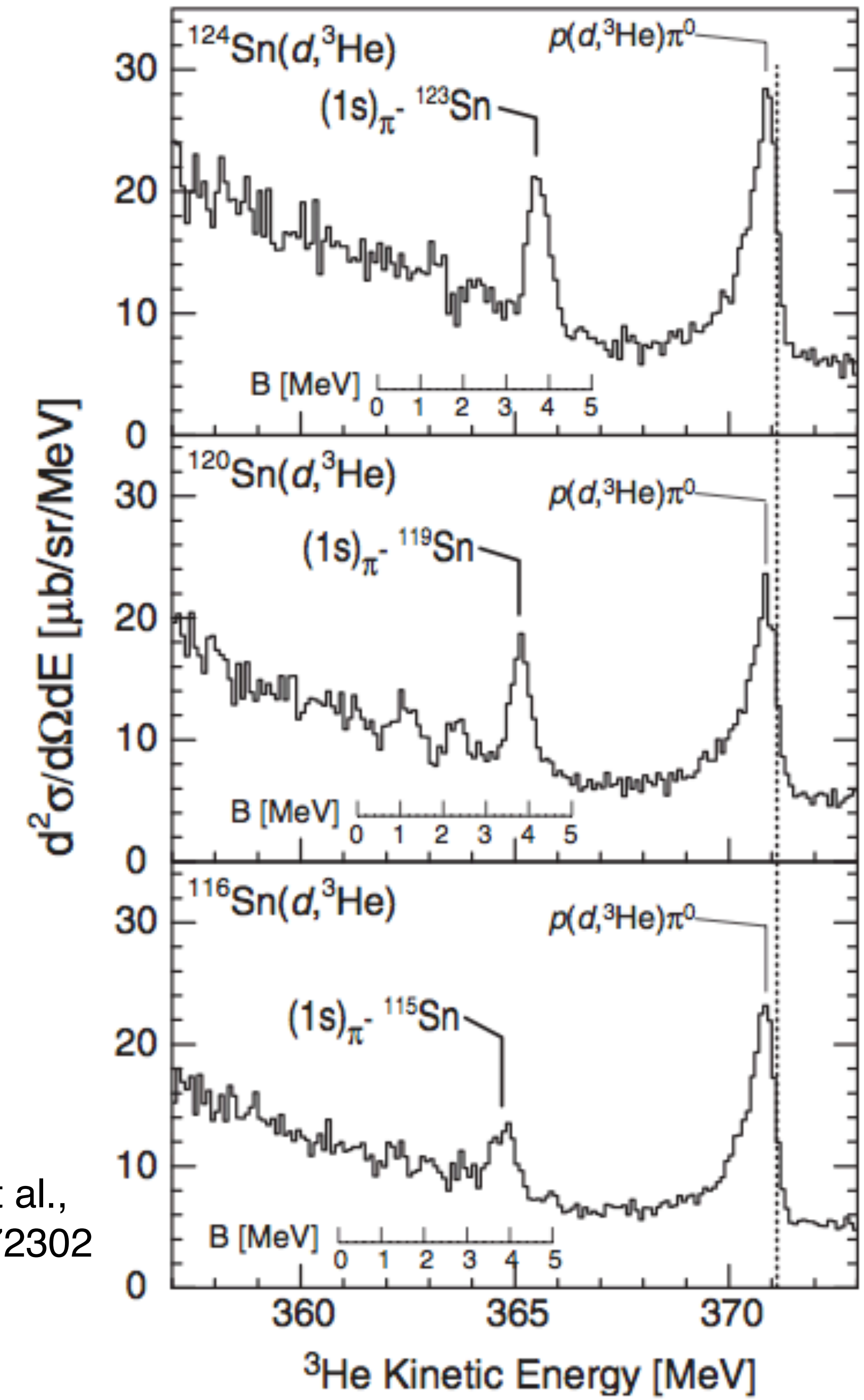

K. Suzuki et al., PRL92(04)072302

Itahashi, K. (2023). Pionic Atoms in Experiment.
In: Tanihata, I., Toki, H., Kajino, T. (eds) Handbook of Nuclear Physics .
Springer, Singapore. https://doi.org/10.1007/978-981-15-8818-1_36-1

Precision experiments at RIKEN-RIBF (2010−)

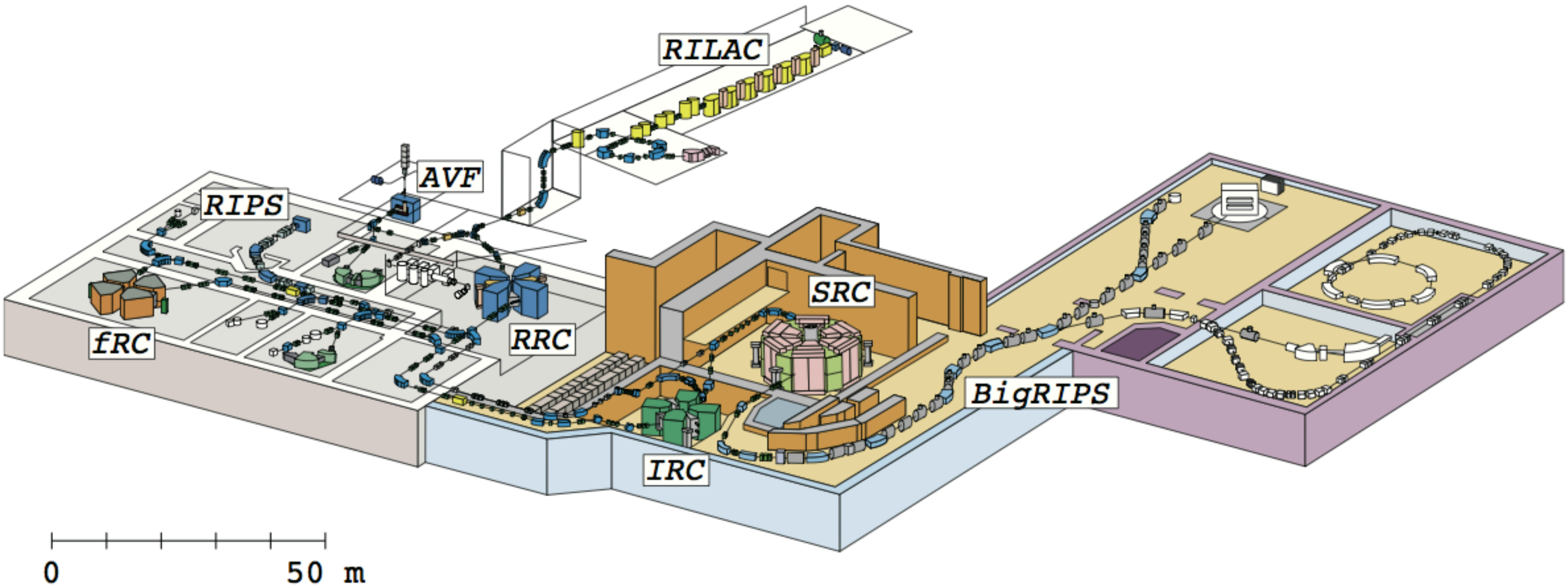

- High intensity deuteron beam (>10^{12}/s) with SRC
- Large acceptance high-resolution spectrometer BigRIPS

Experimental setup

Missing-mass spectroscopy of (d, ^{3}He) reaction

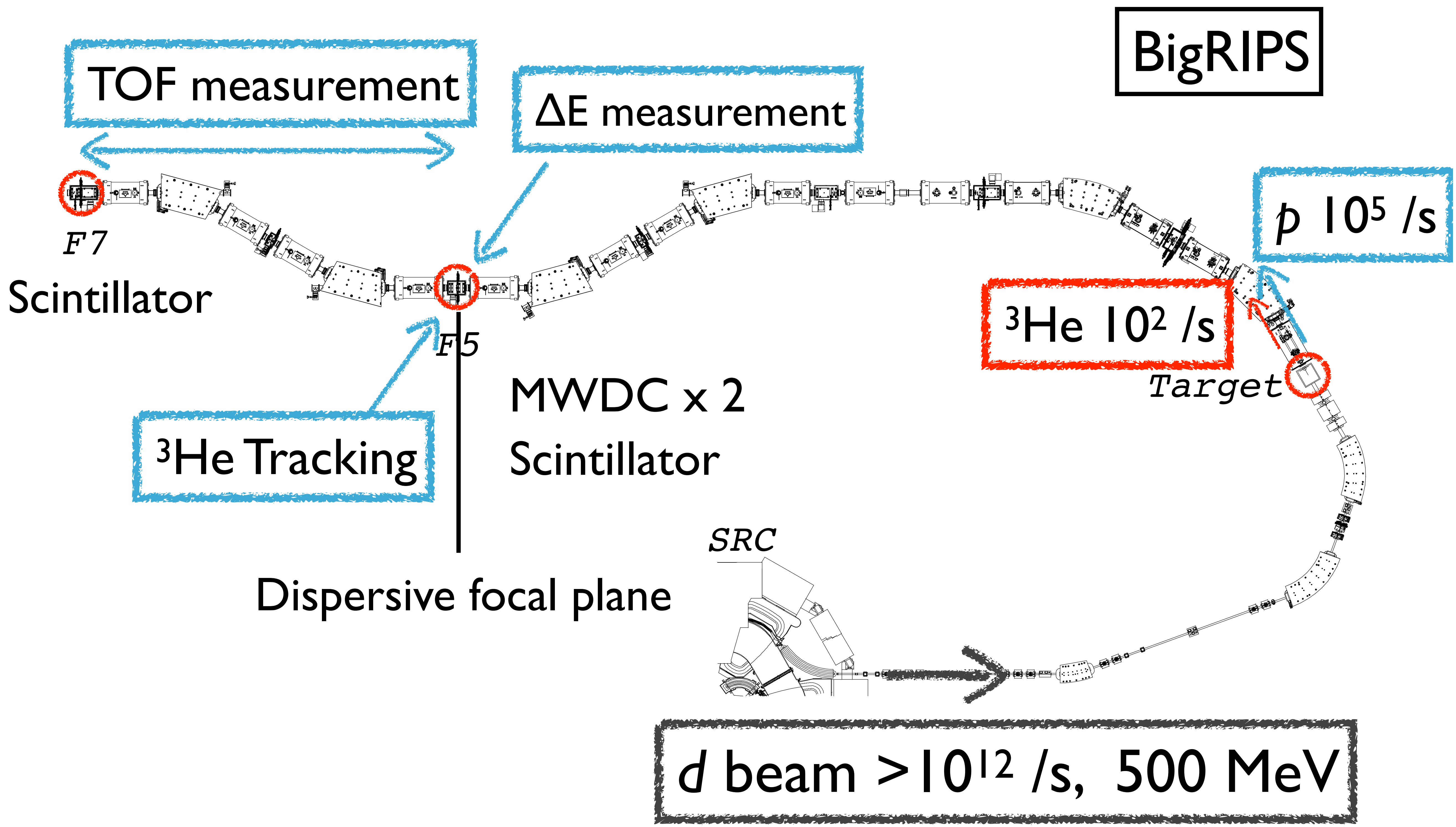

Pilot run with π-^{121}Sn atom (2010)

only 15 hours DAQ

First observation of angle-dependence of π-atom formation cross section

Takahiro Nishi, Kenta Itahashi, et al., Phys. Rev. Lett 120, 152505 (2018)

ΔL ~ R x Δq

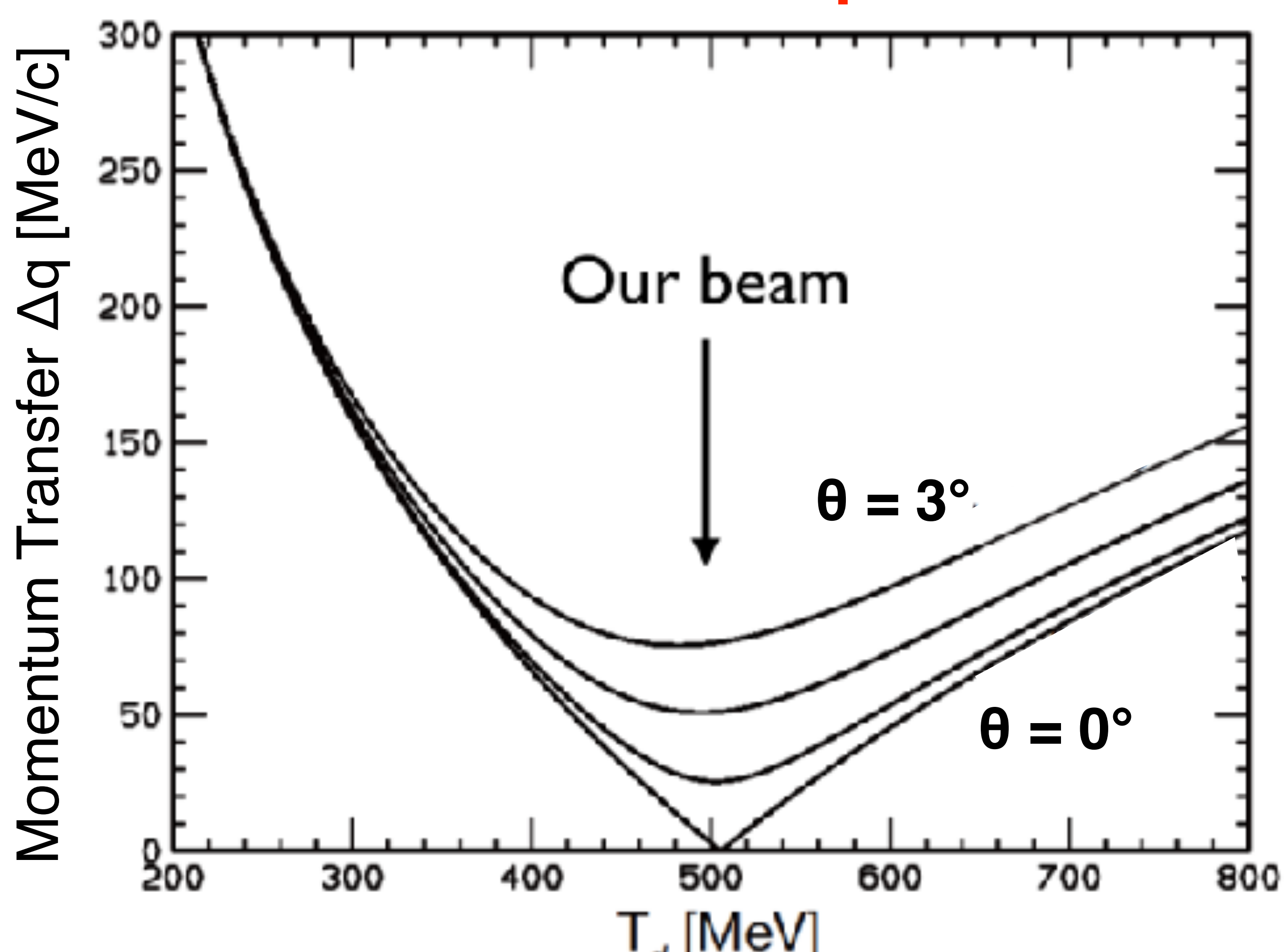

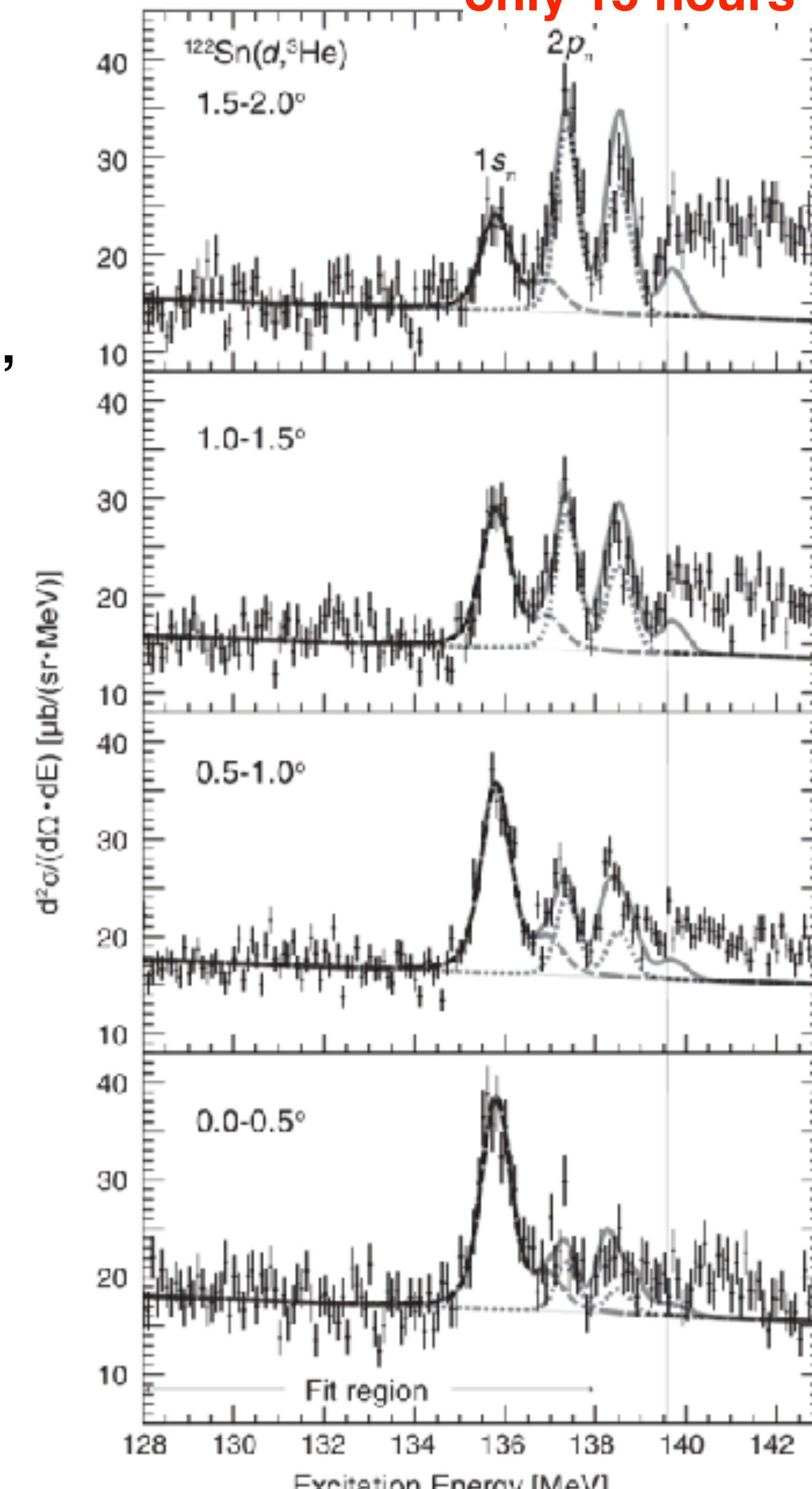

High-precision spectroscopy of π^--^{121}Sn (2014)

piAF collaboration, RIKEN, 2014 May

High-precision spectroscopy of π-^{121}Sn (2014)

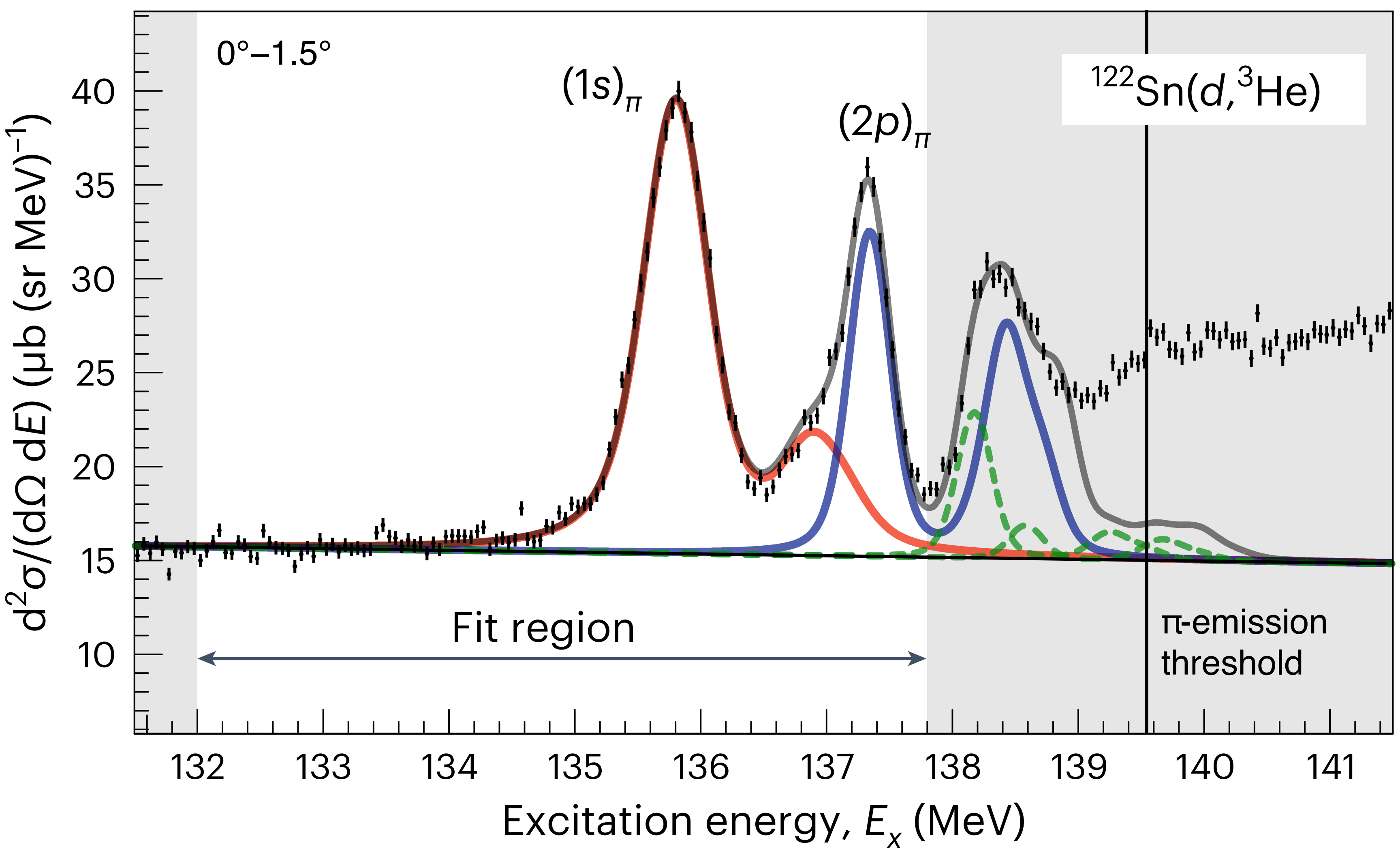

T. Nishi, K. Itahashi, et al.,

Nature Physics (2023)

DOI: 10.1038/s41567-023-02001-x

1s and 2p states observed simultaneously with high-statistics

	Value (keV)	Statistical	Systematic
$B_\pi(1s)$	3,830	±3	+78−76
$B_\pi(2p)$	2,265	±3	+84−83
$B_\pi(1s)-B_\pi(2p)$	1,565	±4	±11
$\Gamma_\pi(1s)$	314	±11	+43−40
$\Gamma_\pi(2p)$	120	±12	+49−28
$\Gamma_\pi(1s)-\Gamma_\pi(2p)$	194	±16	+31−42

Deduction b_1 and chiral condensate at ρ_e

High-precision data
+
updates, corrections
in potential analysis

→ isovector
b1 in medium

Ericson-Ericson potential

$$U_{opt}(r) = U_s(r) + U_p(r),$$

$$U_s(r) = b_0\,\rho + \mathbf{b_1}\,(\rho_n - \rho_p) + B_0\,\rho^2$$

$$U_p(r) = \frac{2\pi}{\mu}\vec{\nabla}\cdot[c(r) + \varepsilon_2^{-1}C_0\rho^2(r)]L(r)\vec{\nabla}$$

- Short range correlation:
- Measured neutron density distribution
- Green's function method for cross section calculation
- Residual interaction
- Neutron spectroscopic factors

N. Ikeno et al., PTEP 2015, 033D01 (2015)
Terashima et al., PHYSICAL REVIEW C 77, 024317 (2008)
Nose-Togawa et al., PRC71, 061601(R) (2005)
Szwec et al., PRC104,054308

T. Nishi, K. Itahashi, et al.,
Nature Physics (2023) DOI: 10.1038/s41567-023-02001-x

Deduction b_1 and chiral condensate at ρ_e

High-precision data
+
updates, corrections
in potential analysis

isovector
b1 in medium

Ericson-Ericson potential

$$U_{opt}(r) = U_s(r) + U_p(r),$$

$$U_s(r) = b_0\,\rho + \mathbf{b_1}\,(\rho_n - \rho_p) + B_0\,\rho^2$$

$$U_p(r) = \frac{2\pi}{\mu}\vec{\nabla}\cdot[c(r) + \varepsilon_2^{-1}C_0\rho^2(r)]L(r)\vec{\nabla}$$

In-vacuum b_1^v Hirtl et al., EPJA57, 70 (2021)

Isovector interaction

-0.15 -0.14 -0.13 -0.12 -0.11 -0.10 -0.09 -0.08 $\mathbf{b_1}$

Result : $b_1 = -0.1163 \pm 0.0056$
at $\rho_e = 0.58\,\rho_0$

In-medium Glashow-Weinberg relation

$$\boxed{\frac{\langle\bar{q}q\rangle^*}{\langle\bar{q}q\rangle} \simeq \left(\frac{b_1}{b_1^*}\right)^{1/2}\left(1 - \gamma\frac{\rho}{\rho_0}\right)}\quad \gamma=0.184\pm0.003$$

Jido, Hatsuda, Kunihiro, PLB670, 109 (2008)

χ-condensate

0.7 0.75 0.8 0.85 0.9 $\langle qq\rangle_e/\langle qq\rangle_0$

theories

T. Nishi, K. Itahashi, et al.,
Nature Physics (2023) DOI: 10.1038/s41567-023-02001-x

Deduced chiral condensate

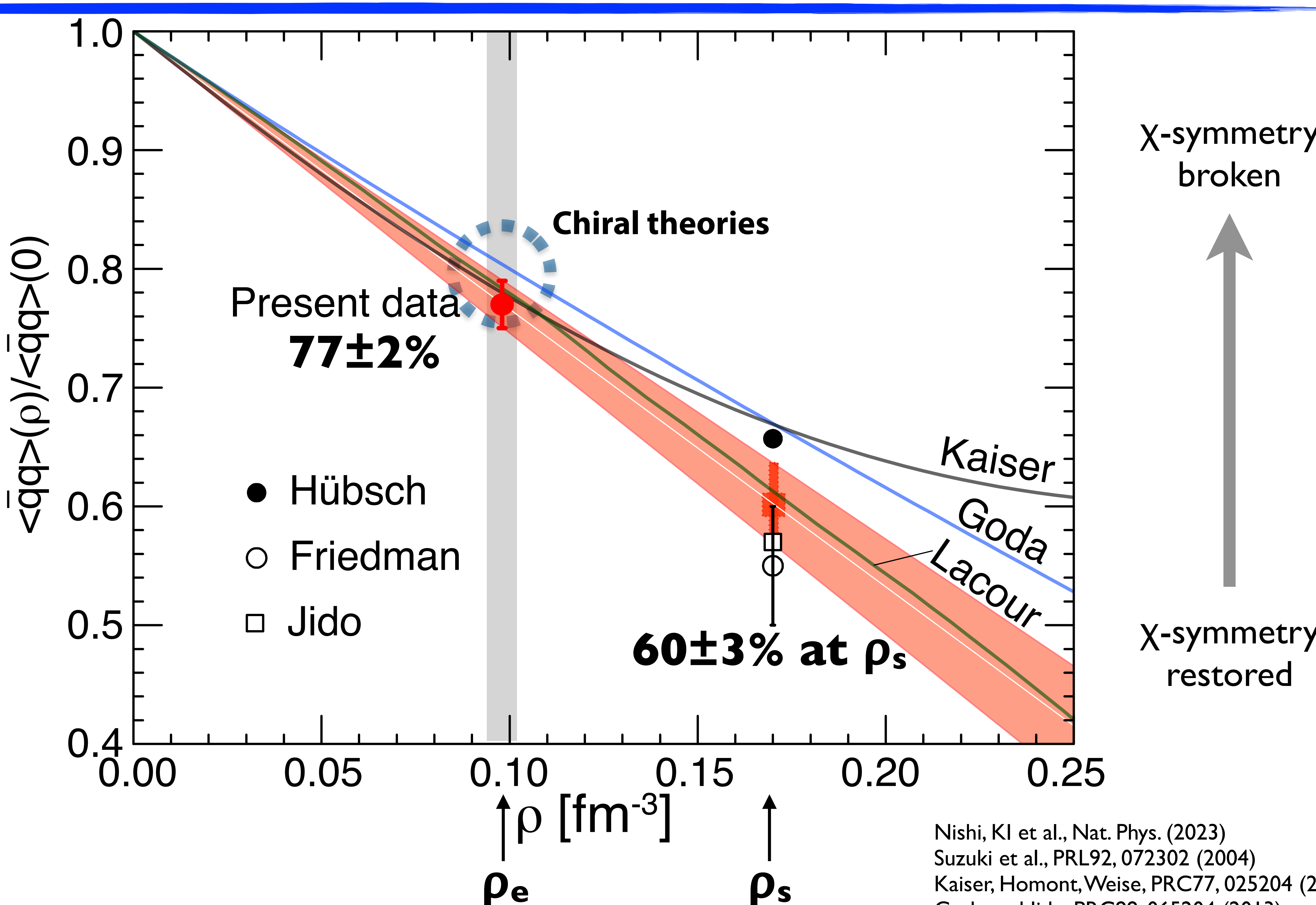

Nishi, KI et al., Nat. Phys. (2023)
Suzuki et al., PRL92, 072302 (2004)
Kaiser, Homont, Weise, PRC77, 025204 (2008)
Goda and Jido, PRC88, 065204 (2013)
Huebsch, Jido, PRC104, 015202 (2021)
Friedman, Gal, PLB792, 340 (2019)
Jido, Hatsuda, Kunihiro, PLB670, 109 (2008)
Lacour, Oller, Meissner, J. Phys. G. 37, 125002 (201

T. Nishi, K. Itahashi, et al.,
Nature Physics (2023) DOI: 10.1038/s41567-023-02001-x

Deduced chiral condensate

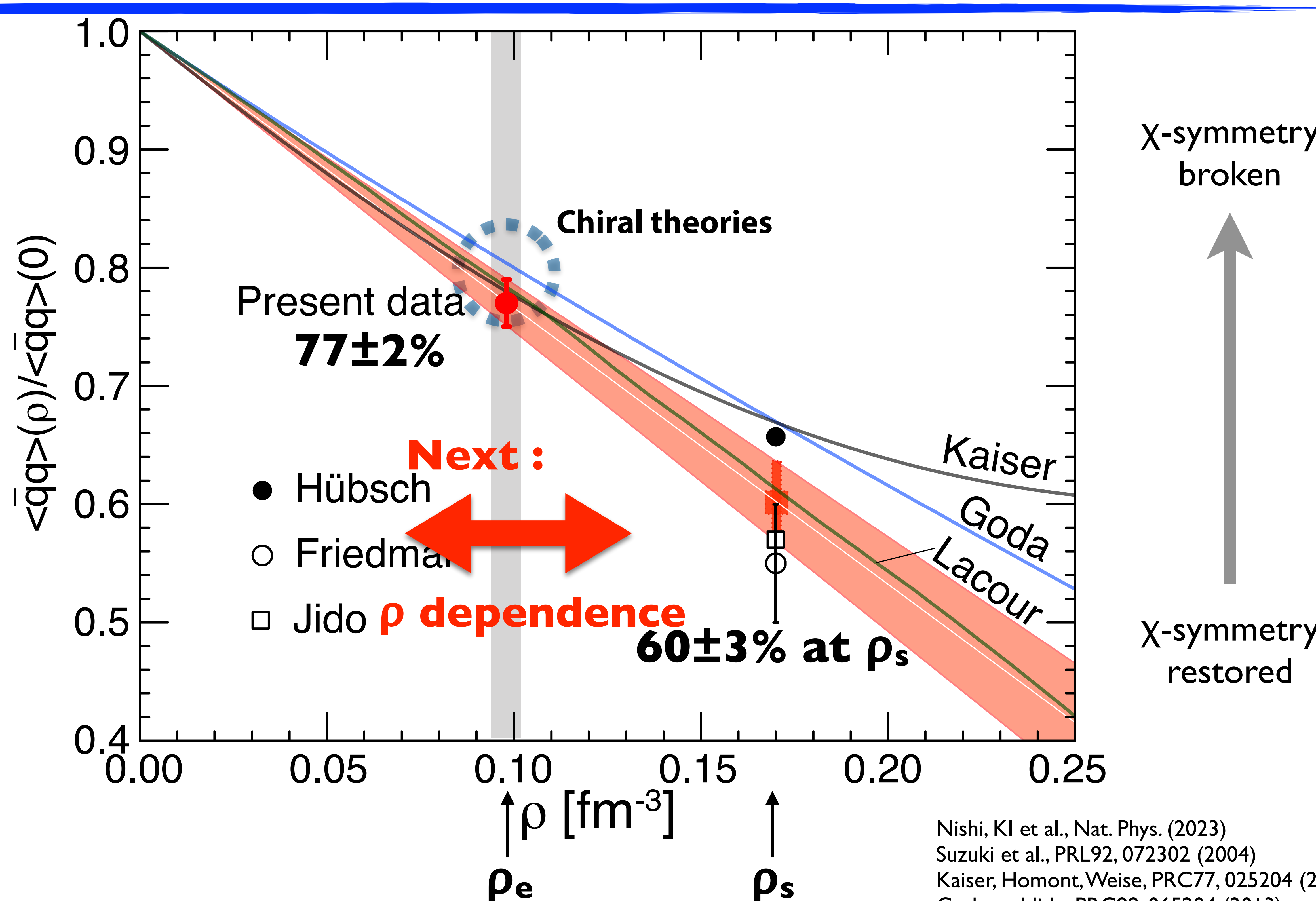

Nishi, KI et al., Nat. Phys. (2023)
Suzuki et al., PRL92, 072302 (2004)
Kaiser, Homont, Weise, PRC77, 025204 (2008)
Goda and Jido, PRC88, 065204 (2013)
Huebsch, Jido, PRC104, 015202 (2021)
Friedman, Gal, PLB792, 340 (2019)
Jido, Hatsuda, Kunihiro, PLB670, 109 (2008)
Lacour, Oller, Meissner, J. Phys. G. 37, 125002 (2010)

T. Nishi, K. Itahashi, et al.,
Nature Physics (2023) DOI: 10.1038/s41567-023-02001-x

Present and future experiments

Precision and systematic spectroscopy (2021)

- □ Sn isotopes from π-^{111}Sn to π-^{123}Sn
- □ aiming at evaluation of ρ-dependence

D(HI, ^{3}He) inverse-kinematics reaction

- □ high-resolution owing to its kinematics
- □ π atom formed in projectile nucleus
  → various beam including unstable nuclei

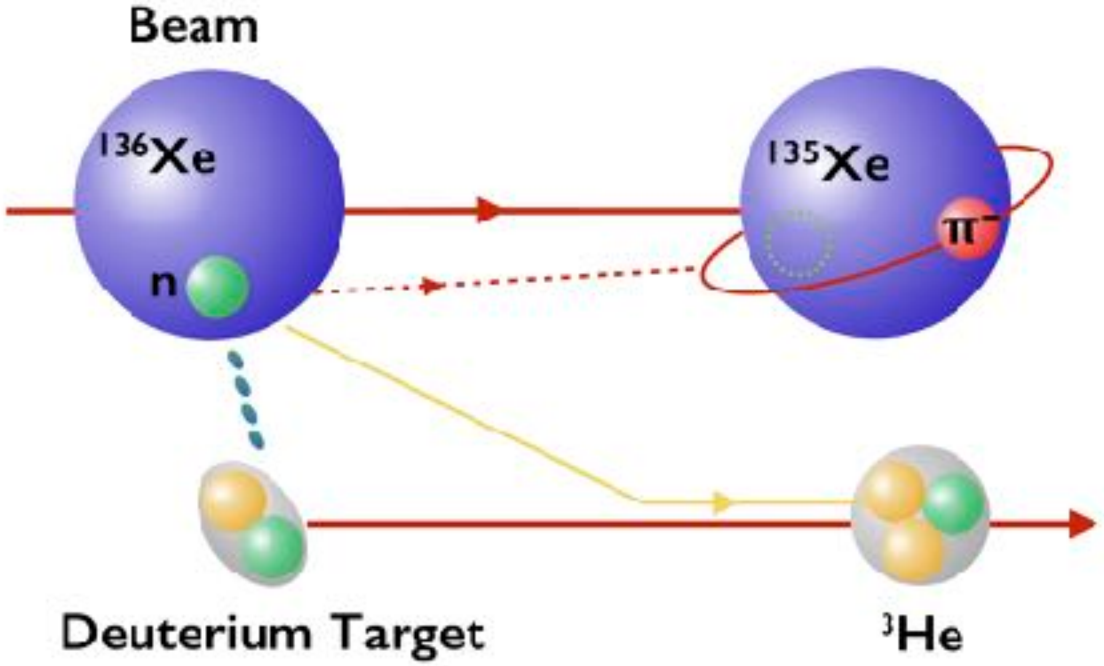

Search for η′-nucleus bound states

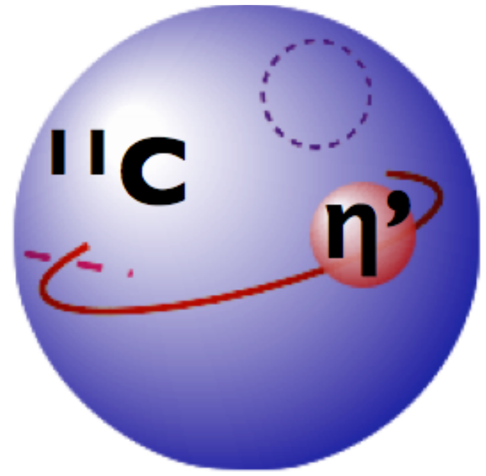

η' meson

η′ meson in vacuum

- Mass = 958 MeV/c² (especially large), Width : 0.2 MeV, $J^P = 0^-$
- $U_A(1)$ anomaly and spontaneous breaking of chiral symmetry

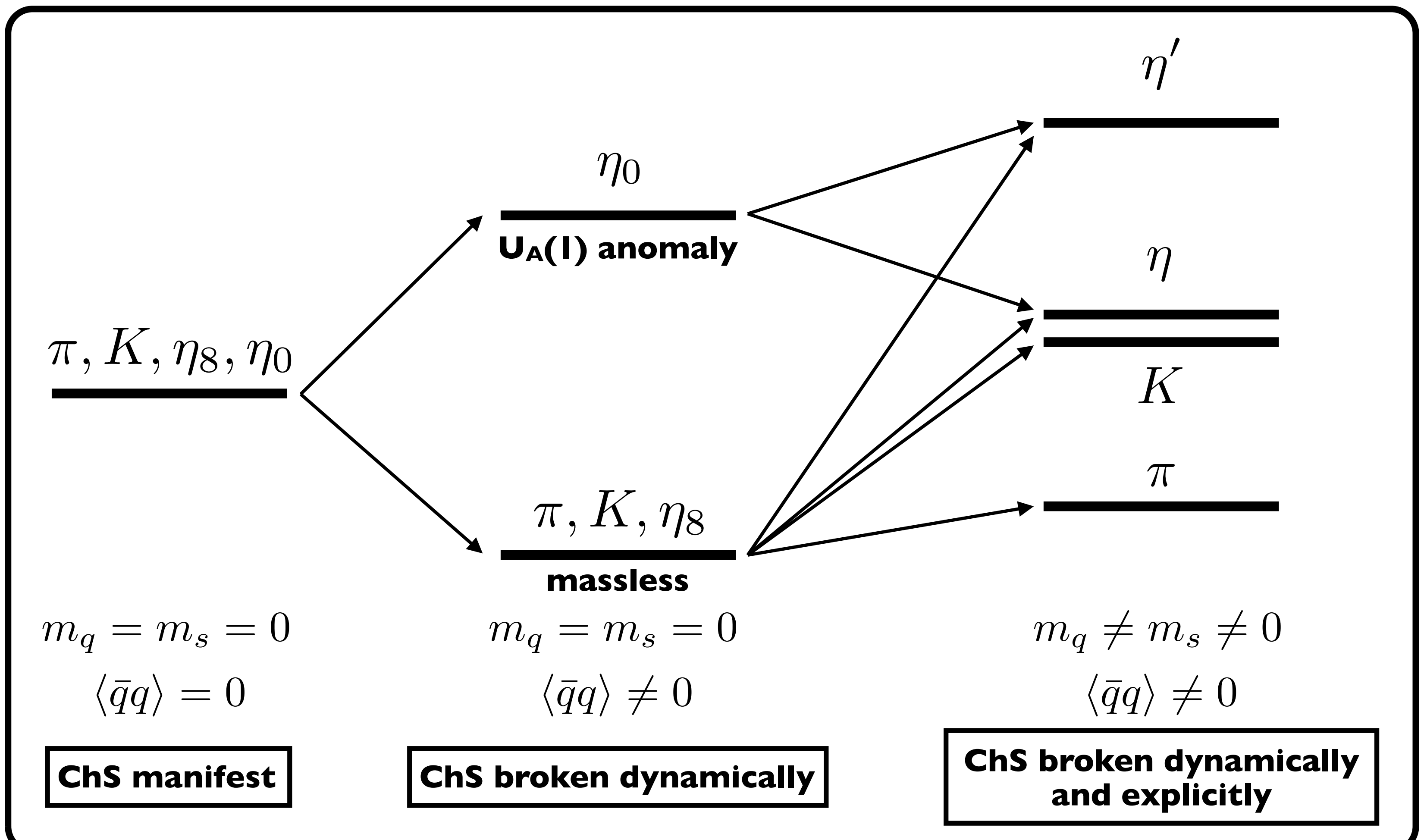

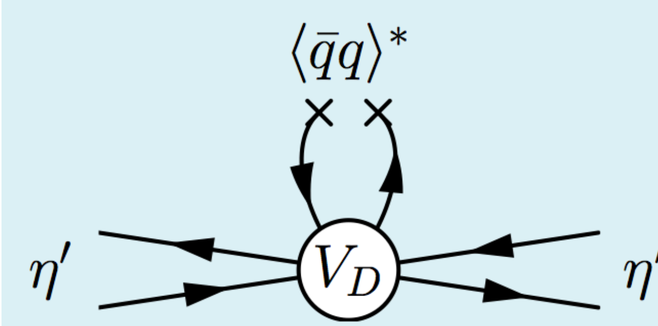

$U_A(1)$ anomaly contributes η' mass through ChSB

H. Nagahiro, D. Jido *et al*, PRC 87, 045201 (2013).

D. Jido, H. Nagahiro, S. Hirenzaki, PRC 85, 032201 (2012).

η′ meson

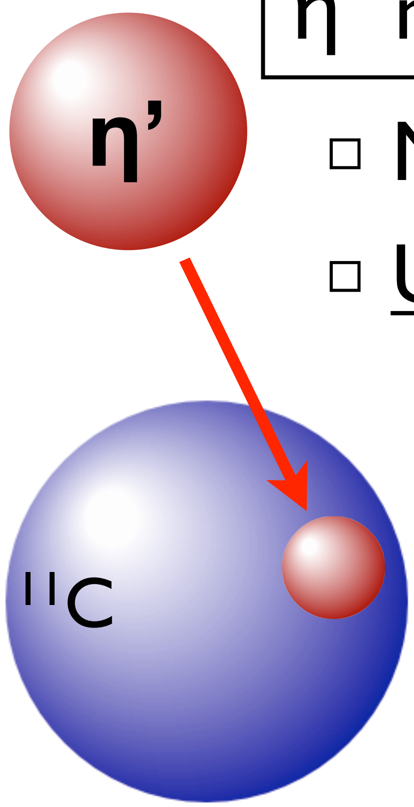

η′ meson in vacuum

- Mass = 958 MeV/c^2 (especially large), Width : 0.2 MeV, $J^P = 0^-$
- $U_A(1)$ anomaly and spontaneous breaking of chiral symmetry

η′ meson at nuclear density

- Partial restoration of chiral symmetry ($\langle \bar{q}q \rangle$ reduced ~ 40%)
- Mass reduction is expected

NJL model

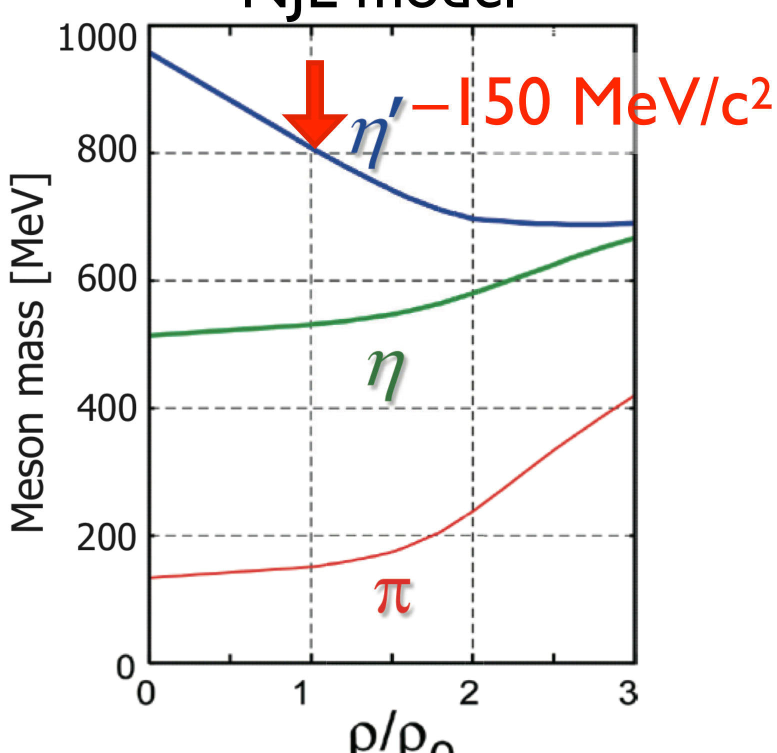

linear σ model

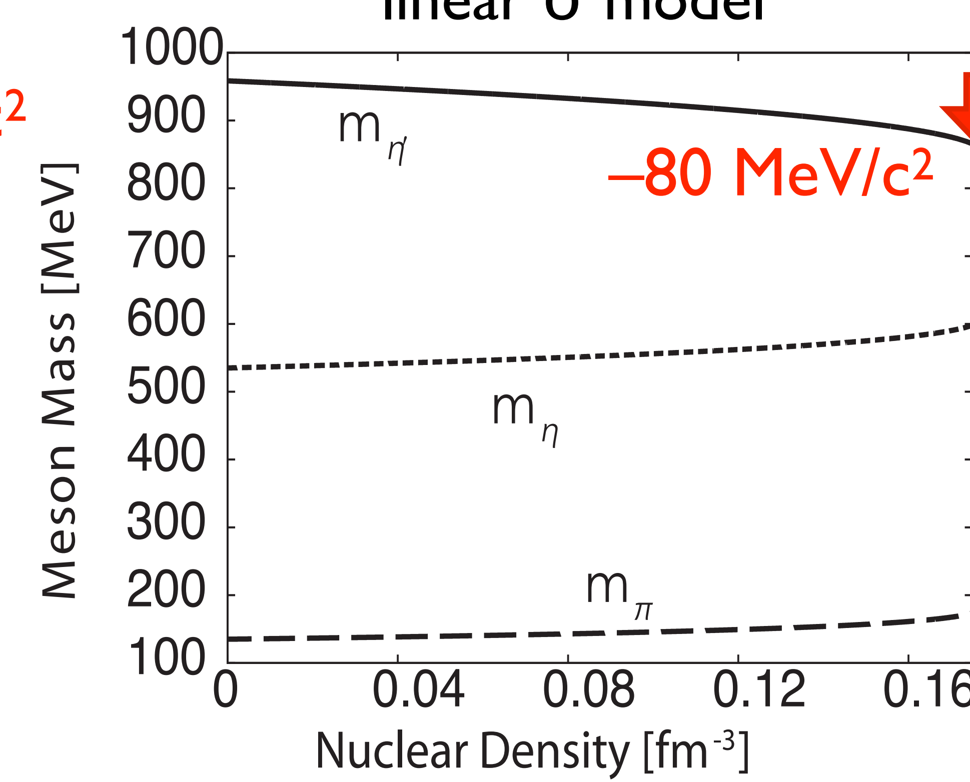

QMC model :
$\Delta m \sim -37$ MeV/c^2
(for $\theta_{\eta\eta'} = -20°$)

H. Nagahiro *et al.*, PRC 74, 045203(2006).
S. Sakai *et al.*, D. Jido, PRC 88, 064906 (2013).
S.D. Bass, A.W. Thomas, PLB 634, 368 (2006).

η'-nucleus potential

η'-nucleus optical potential :

$$V_{\eta'} = (V_0 + iW_0)\frac{\rho(r)}{\rho_0}$$

$$V_0 = \Delta m(\rho_0),\quad W_0 = -\Gamma(\rho_0)/2$$

Theoretical predictions

$\Delta m(\rho_0) \sim -150\ \mathrm{MeV}/c^2$ (NJL), $-80\ \mathrm{MeV}/c^2$ (linear σ), $-37\ \mathrm{MeV}/c^2$ (QMC)

H. Nagahiro *et al.*, PRC 74, 045203(2006).
S. Sakai, D. Jido, PRC 88, 064906 (2013).
S.D. Bass, A.W. Thomas, PLB 634, 368 (2006)

Experimental indications (CBELSA/TAPS)

- $V_0 \sim -40$ MeV (excitation function, mom. distribution)
- $W_0 = -13 \pm 3(\mathrm{stat}) \pm 3(\mathrm{syst})$ MeV (transparency ratio)

M. Nanova *et al.*, PRC 94 025205 (2016)
M. Nanova *et al.*, PLB 727, 417 (2013).
M. Nanova *et al.*, PLB 710, 600 (2012).
S. Friedrich *et al.*, EPJA 52, 297 (2016).

η′-nucleus potential

η′-nucleus optical potential :

$$V_{\eta'} = (\underline{V_0} + i\underline{W_0}) \frac{\rho(r)}{\rho_0}$$

$V_0 = \Delta m(\rho_0)$, $W_0 = -\Gamma(\rho_0)/2$

Theoretical predictions

$\Delta m(\rho_0) \sim -150$ MeV/c^2 (NJL), -80 MeV/c^2 (linear σ), -37 MeV/c^2 (QMC)

H. Nagahiro *et al.*, PRC 74, 045203(2006).
S. Sakai, D. Jido, PRC 88, 064906 (2013).
S.D. Bass, A.W. Thomas, PLB 634, 368 (2006)

Experimental indications (CBELSA/TAPS)

- $V_0 \sim -40$ MeV (excitation function, mom. distribution)
- $W_0 = -13 \pm 3$(stat) ± 3(syst) MeV (transparency ratio)

M. Nanova *et al.*, PRC 94 025205 (2016)
M. Nanova *et al.*, PLB 727, 417 (2013).
M. Nanova *et al.*, PLB 710, 600 (2012).
S. Friedrich *et al.*, EPJA 52, 297 (2016).

η'p scattering length

$\boxed{pp \to pp\eta'}$: $\mathrm{Re}(a_{\eta' p}) = 0 \pm 0.43$ fm, $\mathrm{Im}(a_{\eta' p}) = 0.37^{+0.40}_{-0.16}$ fm

E. Czerwiński et al., PRL 113, 062004 (2014)

$\boxed{\gamma p \to p\eta'}$: $|a_{\eta' p}| = 0.403 \pm 0.015 \pm 0.060$ fm, $\delta = (87 \pm 2)^\circ$

A. V. Anisovich et al., PLB 785 (2018) 626

Direct experimental study is needed.
If $|W_0| < |V_0|$ → possibility of observing bound states

Experimental search for η'-mesic nuclei

$^{12}C(p,d)$ missing-mass spectroscopy at GSI

2.5 GeV proton

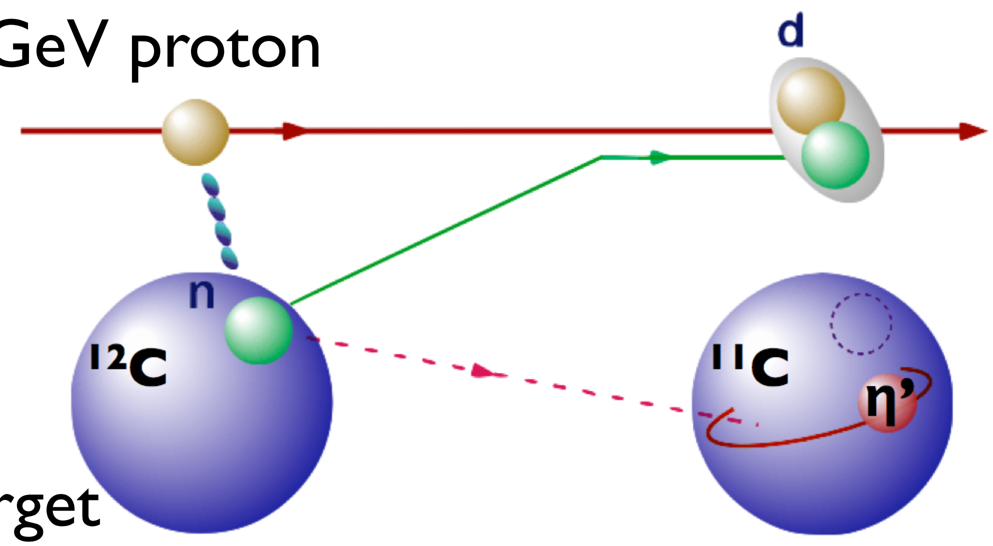

Target

Y. K. Tanaka, K. Itahashi, H. Fujioka *et al,*
Phys. Rev. Lett. 117, 202501 (2016)

Excitation spectrum

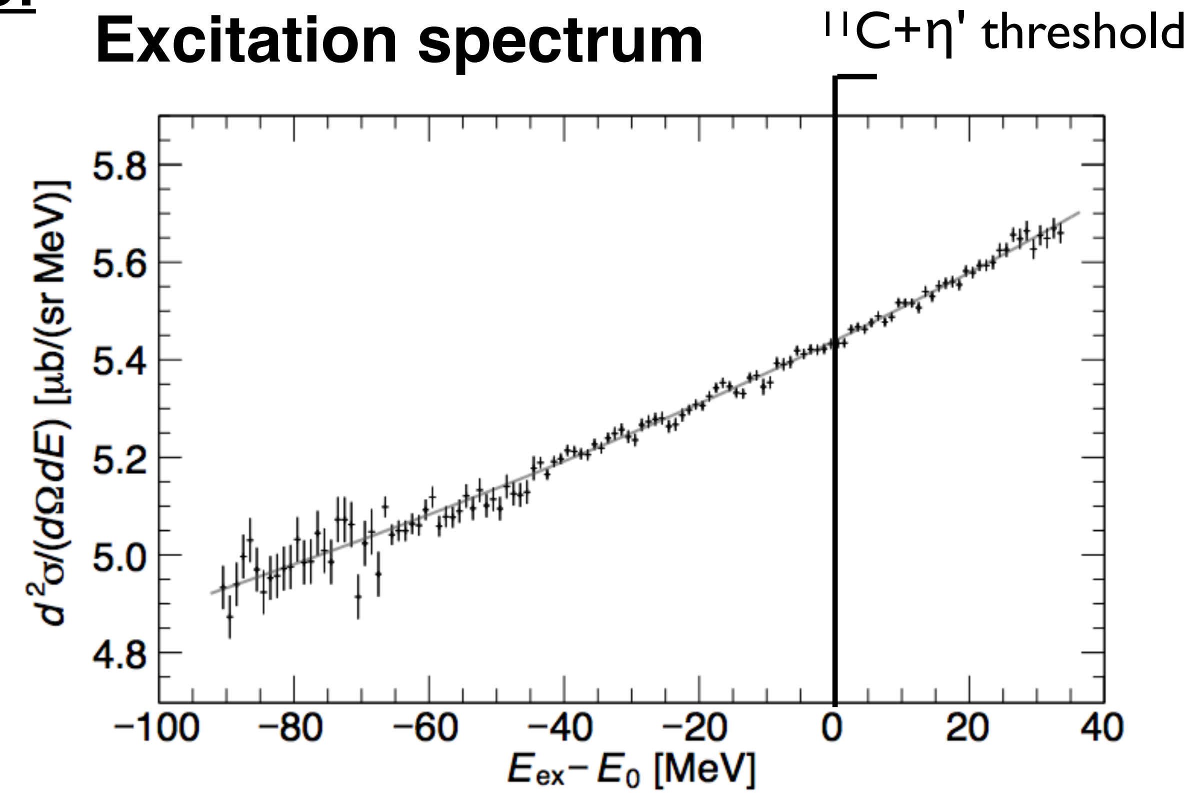

Experimental search for η'-mesic nuclei

$^{12}C(p,d)$ missing-mass spectroscopy at GSI

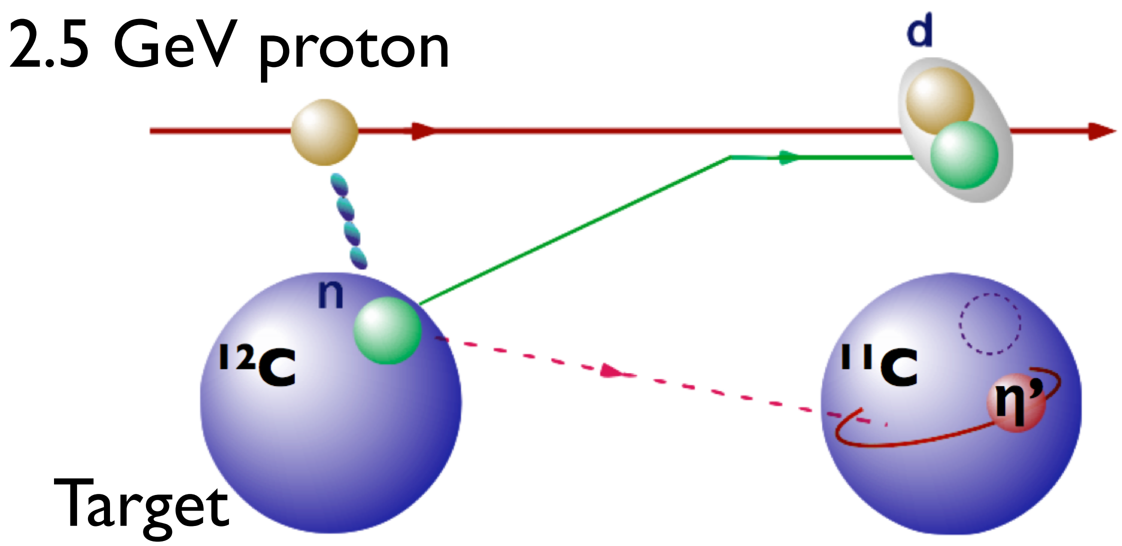

Y. K. Tanaka, K. Itahashi, H. Fujioka *et al,* Phys. Rev. Lett. 117, 202501 (2016)

Upper limit of cross section & Constraint on potential (V_0,W_0)

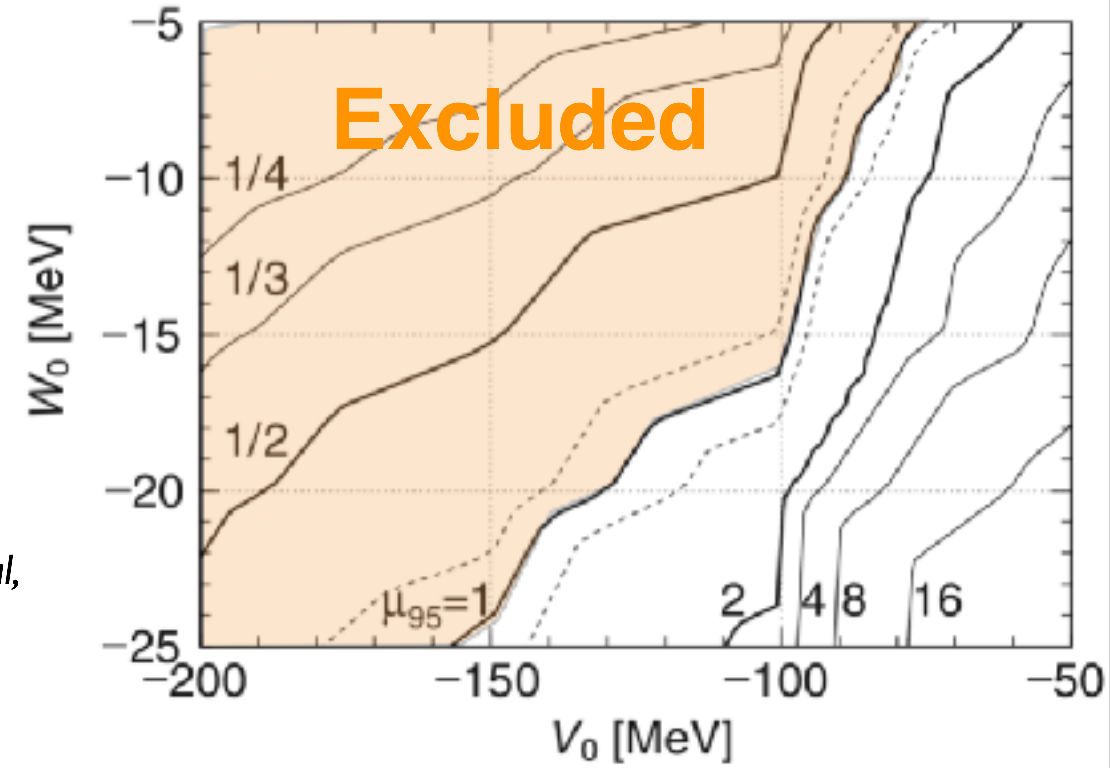

Experimental search for η'-mesic nuclei

^{12}C(*p*,*d*) missing-mass spectroscopy at GSI

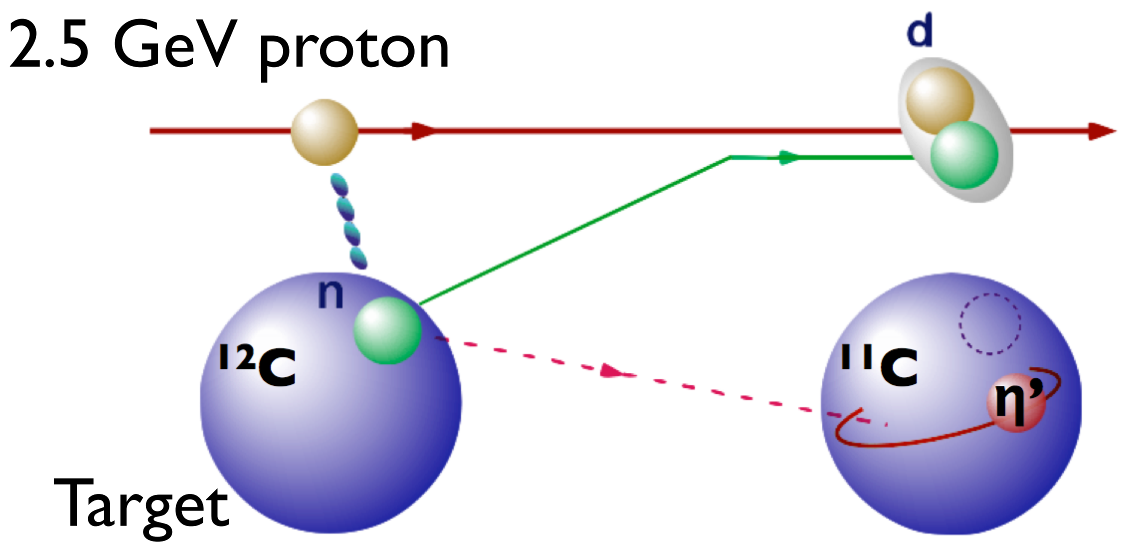

Y. K. Tanaka, K. Itahashi, H. Fujioka *et al*, Phys. Rev. Lett. 117, 202501 (2016)

Upper limit of cross section & Constraint on potential (V_0,W_0)

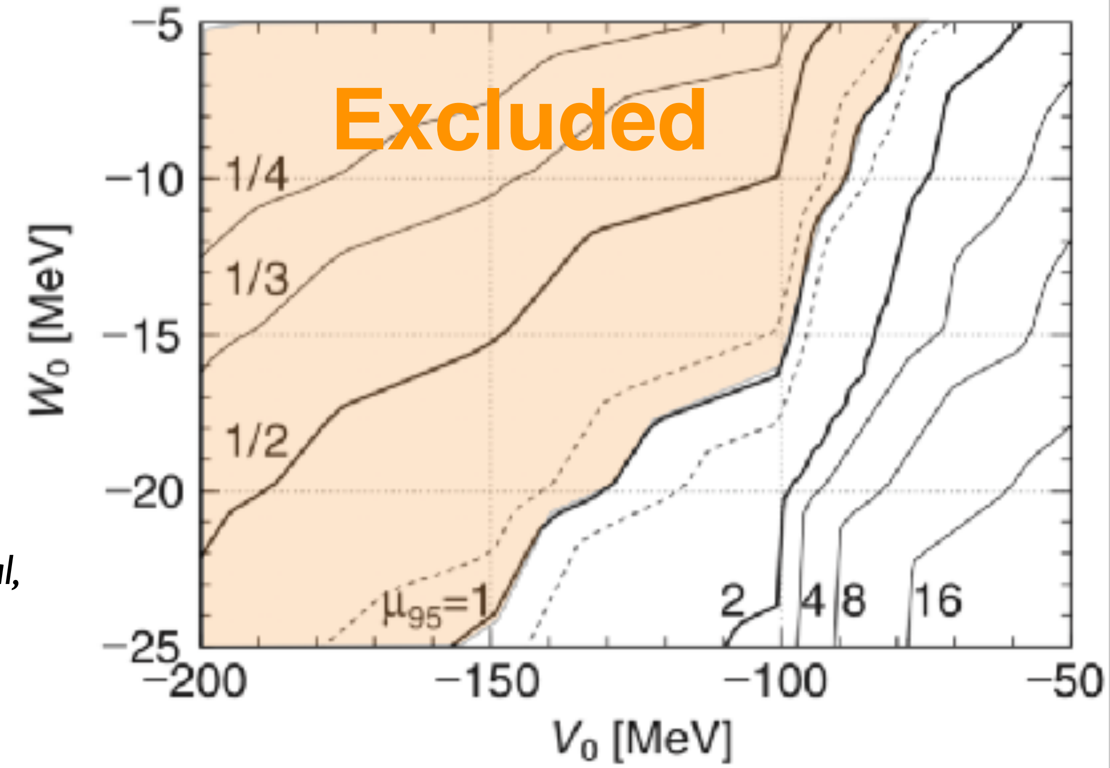

^{12}C(γ,*p*) reaction at LEPS2/Spring8

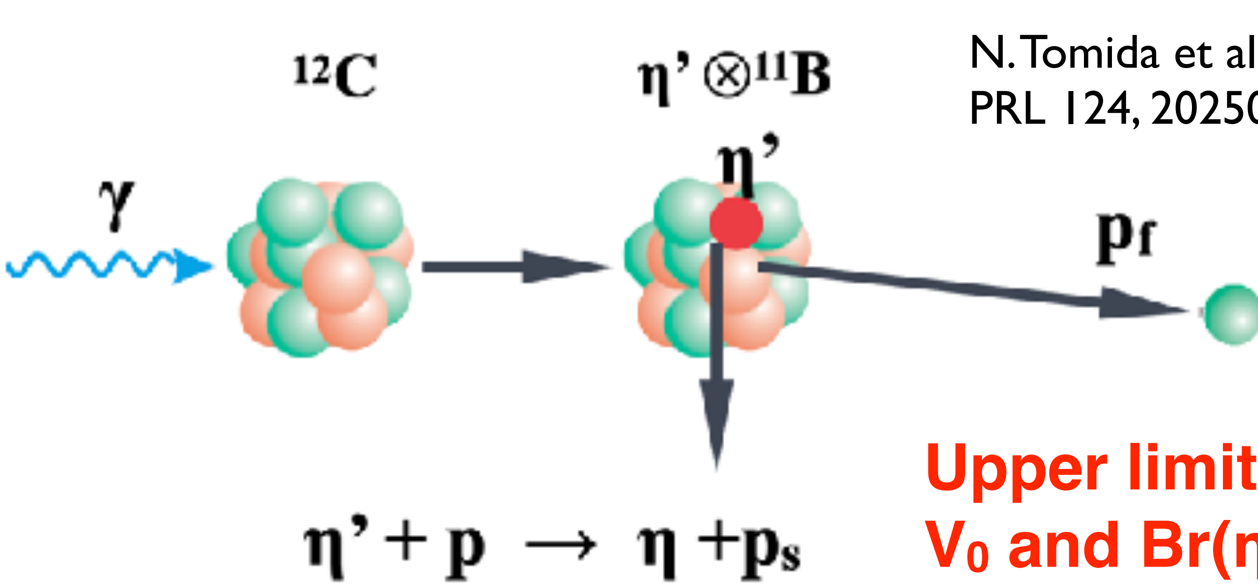

N. Tomida et al., PRL 124, 202501 (2020)

Upper limit on V_0 and Br(η'N→ηN) for W_0 = -12 MeV

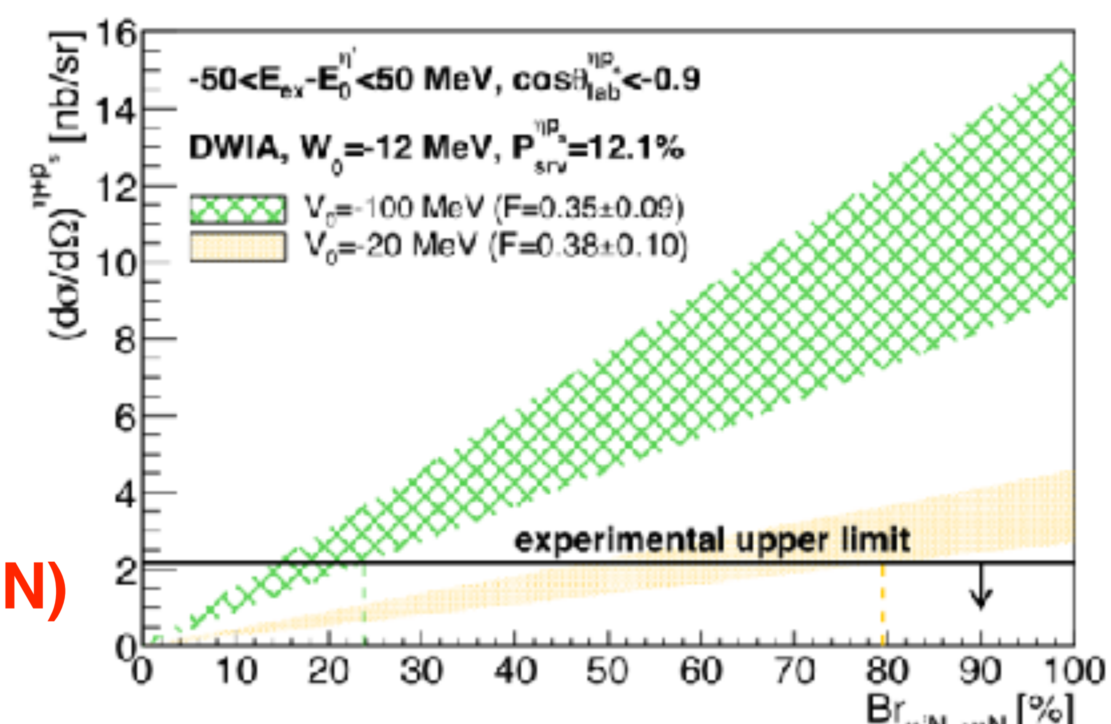

Related talk by N. Muramatsu

Experimental search for η'-mesic nuclei

$^{12}C(p,d)$ missing-mass spectroscopy at GSI

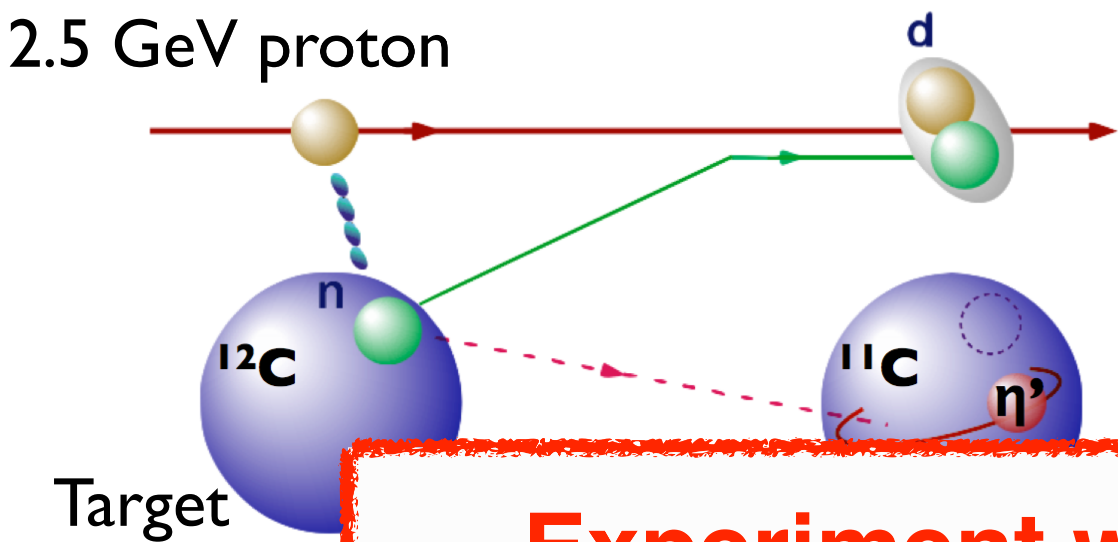

Upper limit of cross section & Constraint on potential (V_0,W_0)

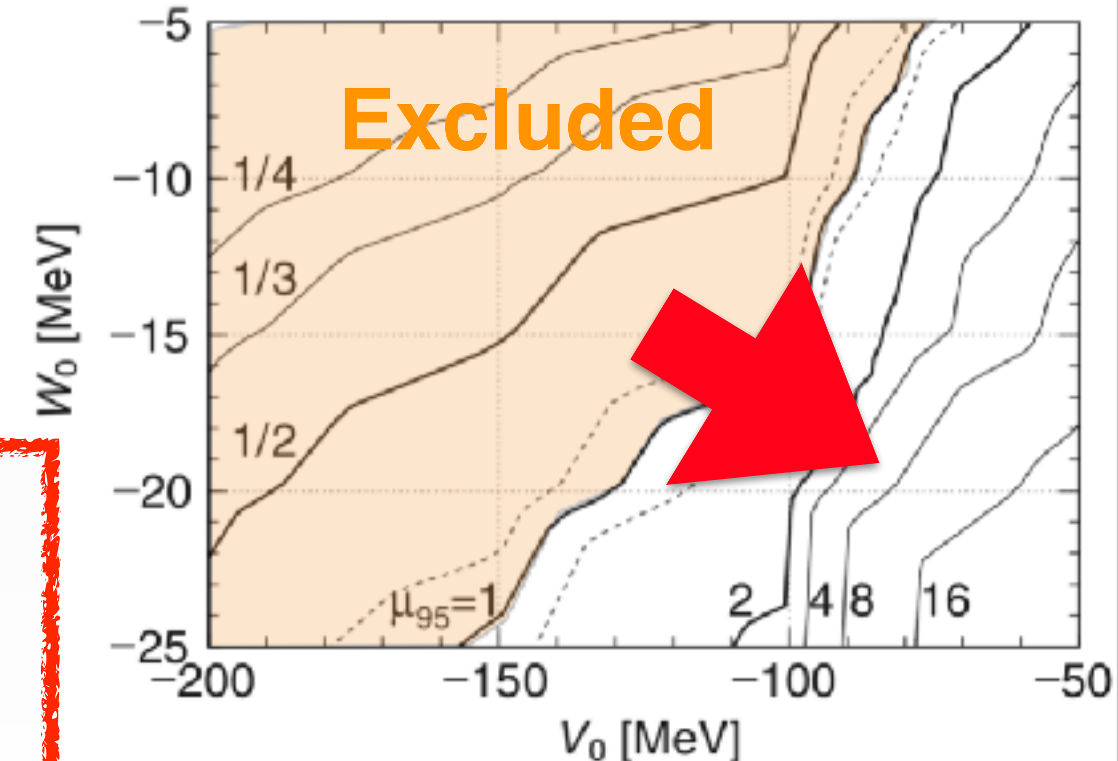

Experiment with higher sensitivity necessary !

$^{12}C(\gamma,p)$ r

N. Tomida et al.,
PRL 124, 202501 (2020)

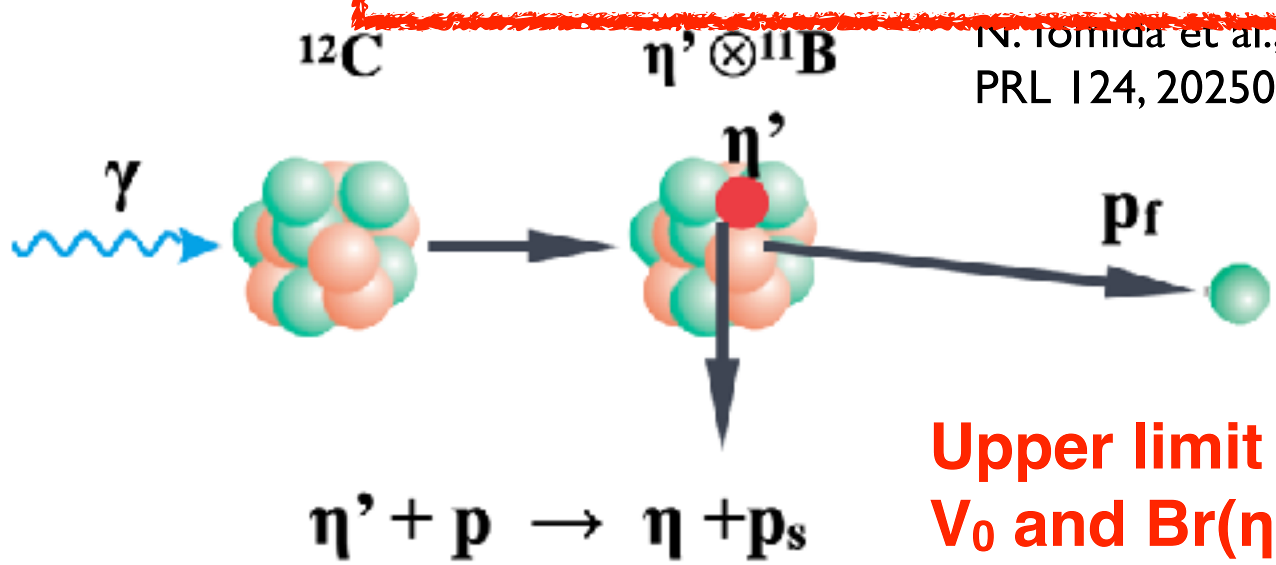

Upper limit on V_0 and Br(η'N→ηN) for W_0 = -12 MeV

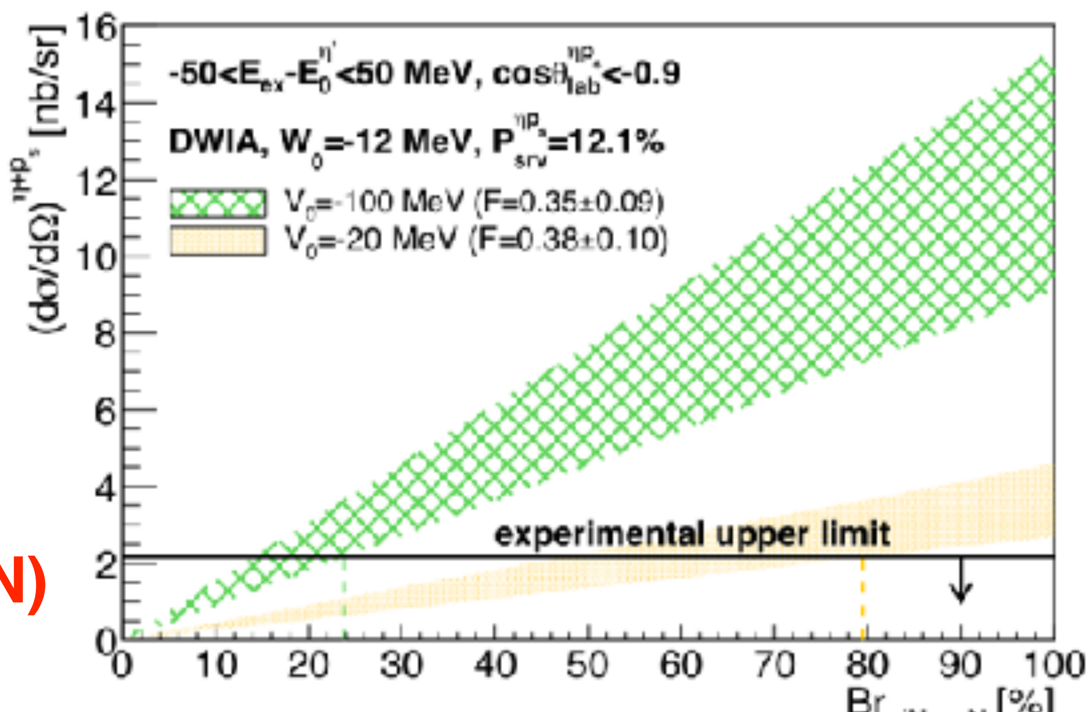

Related talk by N. Muramatsu

Semi-exclusive experiment at GSI/FAIR

Background

multi-π production

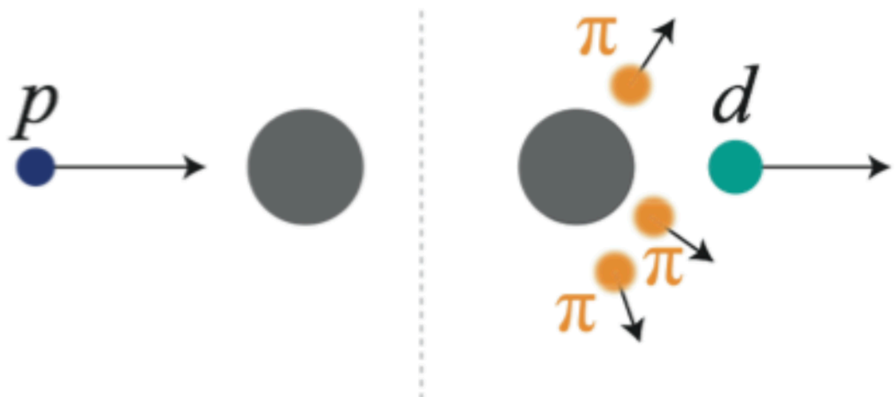

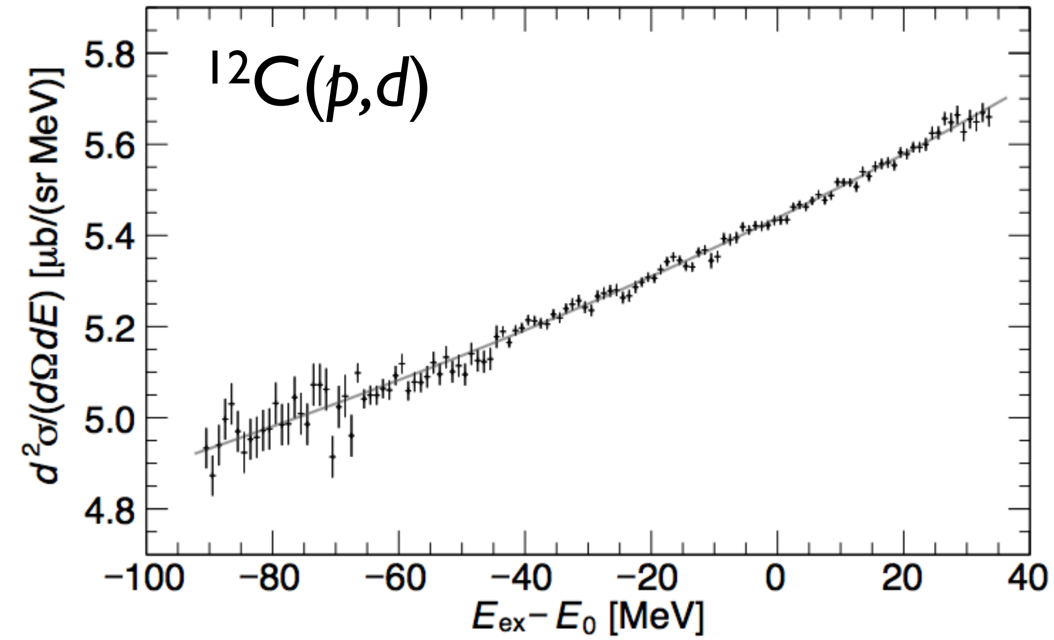

Signal

η′-mesic nuclei formation

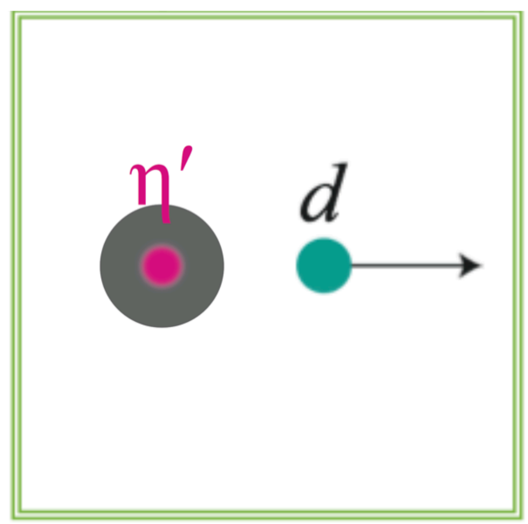

Semi-exclusive experiment at GSI/FAIR

Background

multi-π

production

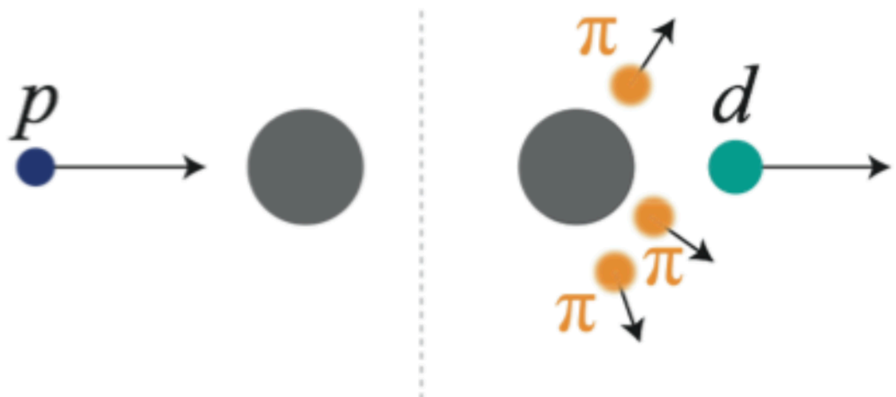

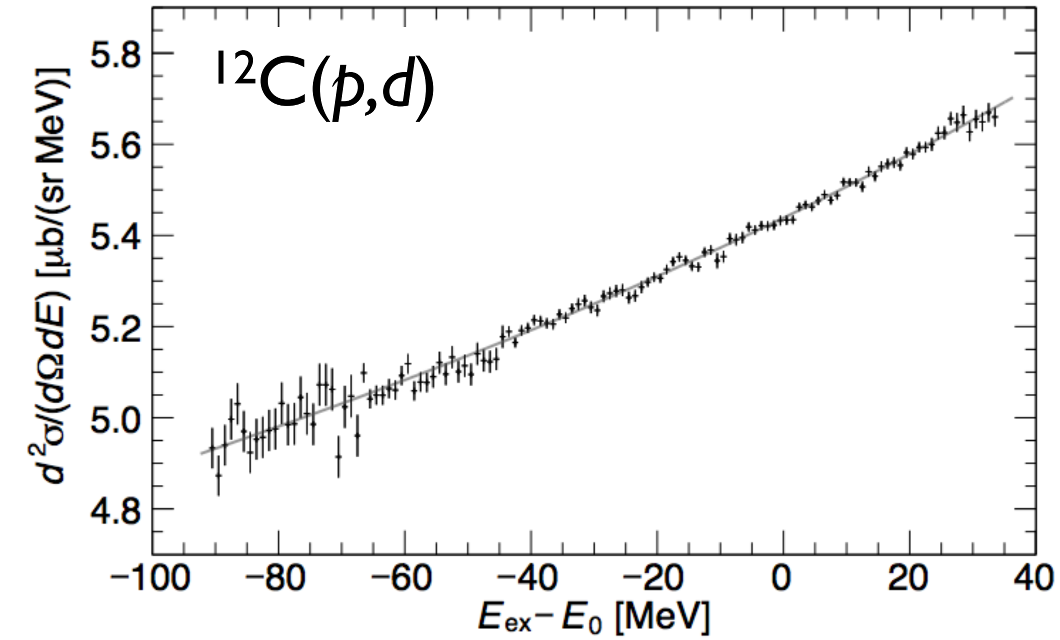

Signal

η′-mesic nuclei

formation

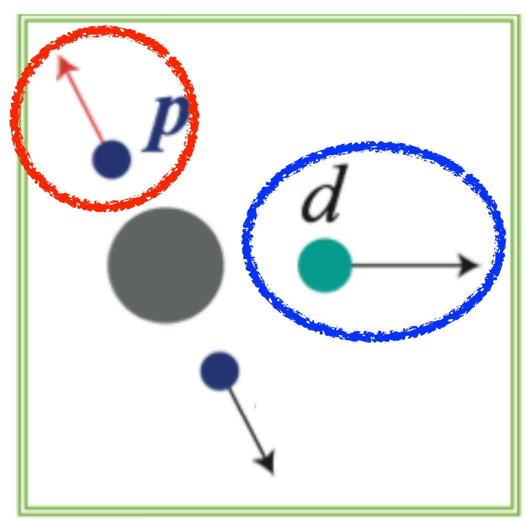

η'NN→NN, *η'N→ηN, πN,...*

H. Nagahiro, Nucl. Phys. A **914**, 360 (2013).

Coincidence measurement of
decay proton and forward deuteron

Semi-exclusive experiment at GSI/FAIR

Background

multi-π production

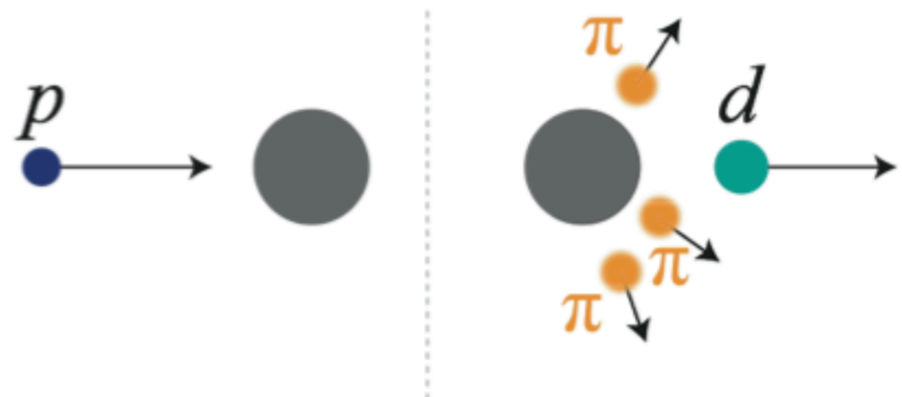

Signal

η′-mesic nuclei formation

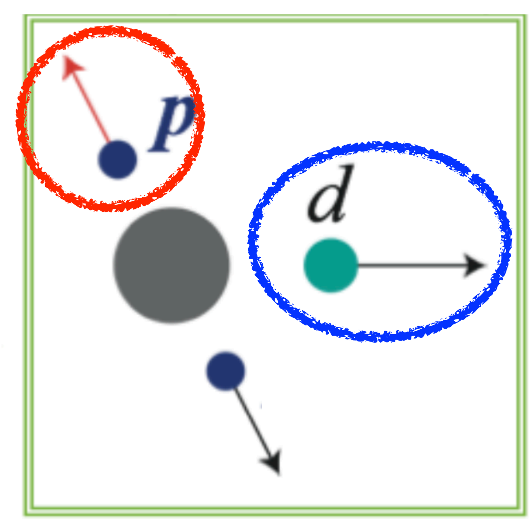

$\eta' NN \rightarrow NN$, $\eta' N \rightarrow \eta N$, πN,...

H. Nagahiro, Nucl. Phys. A **914**, 360 (2013).

Calculation by microscopic transport model (JAM)

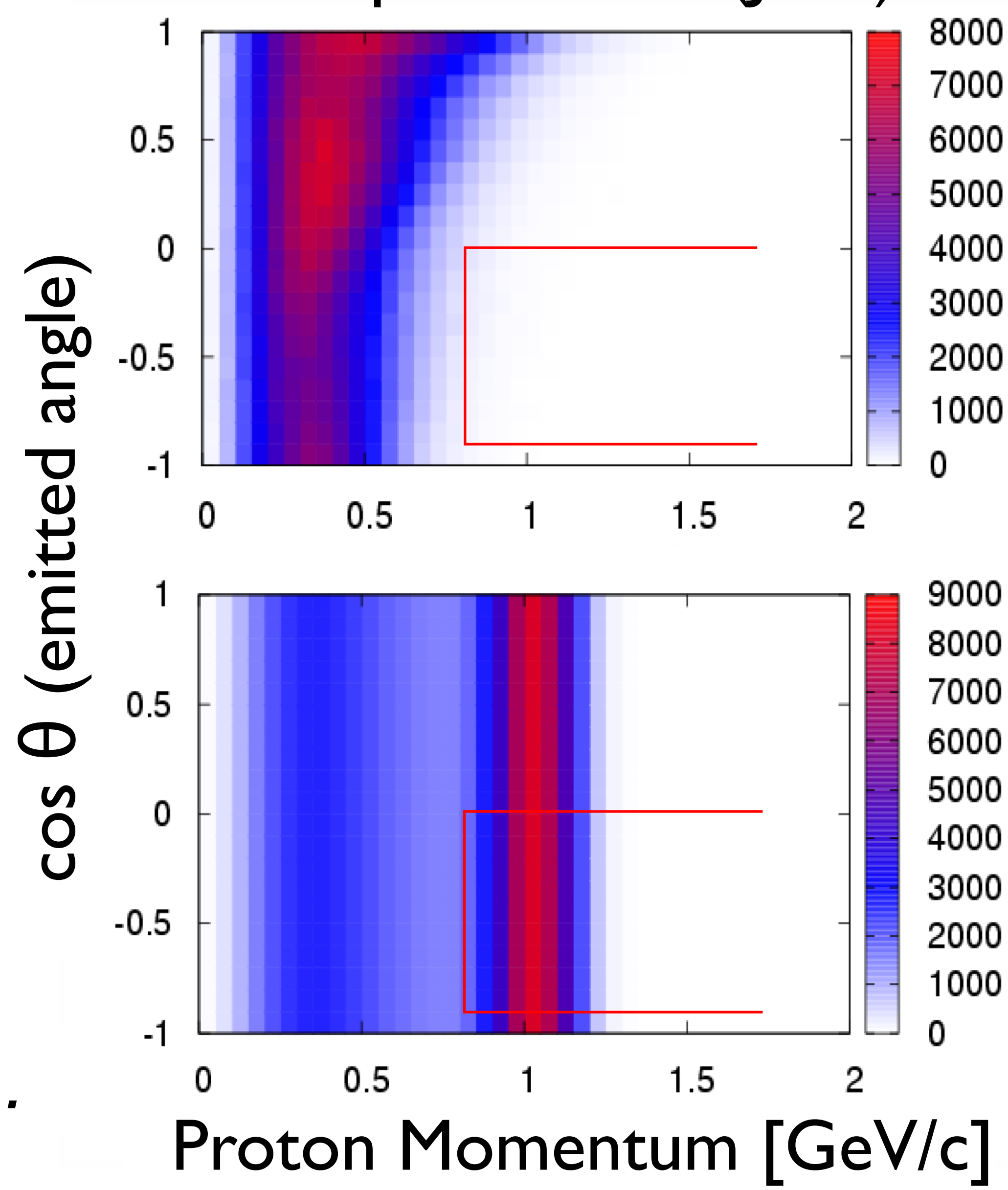

Y. Higashi

Coincidence measurement of decay proton and forward deuteron

~ 100 improvement in Signal / BG ratio

Semi-exclusive experiment at GSI/FAIR

Background

multi-π production

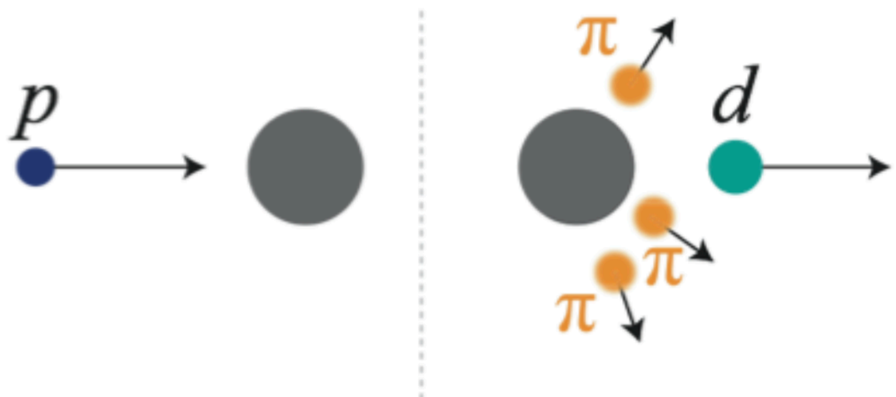

Signal

η′-mesic nuclei formation

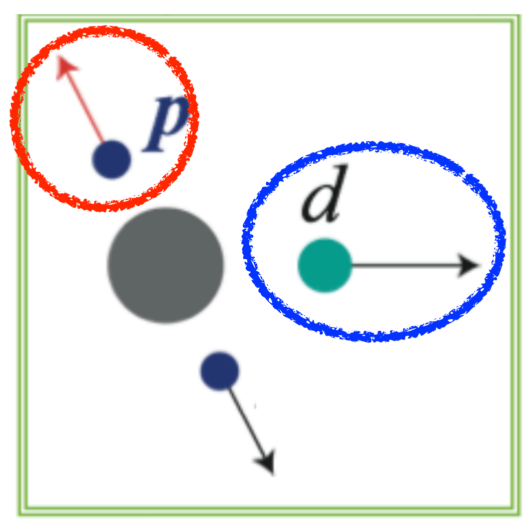

η'NN→NN, η'N→ηN, πN,...

H. Nagahiro, Nucl. Phys. A **914**, 360 (2013).

Simulated spectrum with backward proton tagging

(V_0,W_0) = (-90,-17) MeV

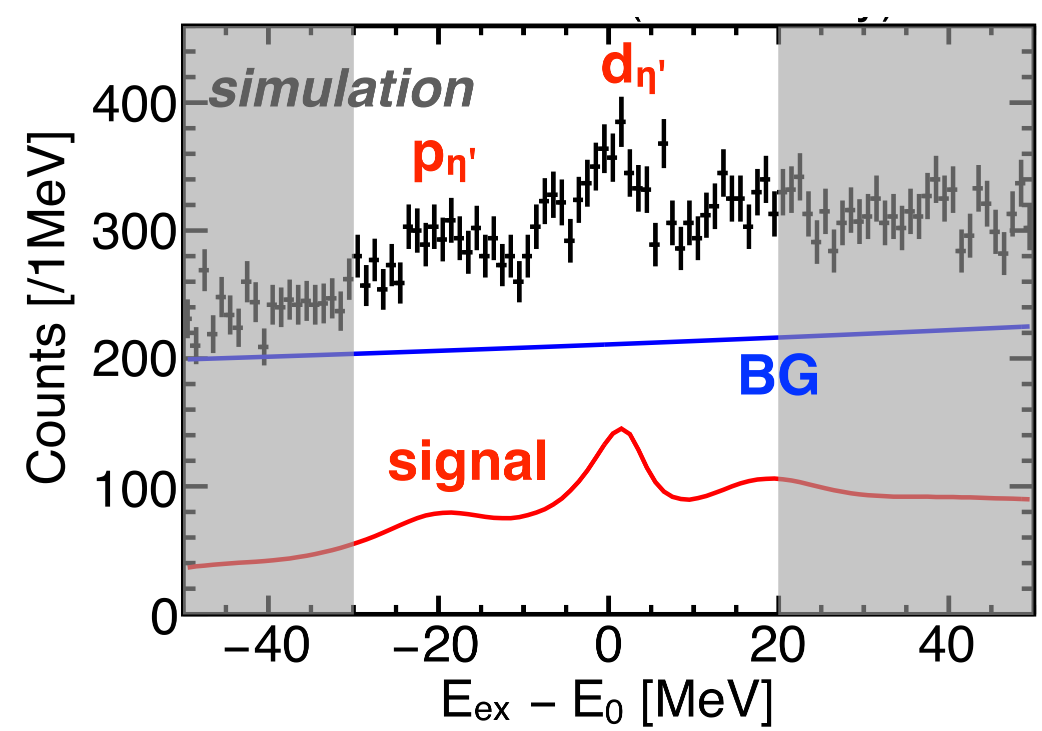

Coincidence measurement of decay proton and forward deuteron

WASA-FRS beam time in 2022

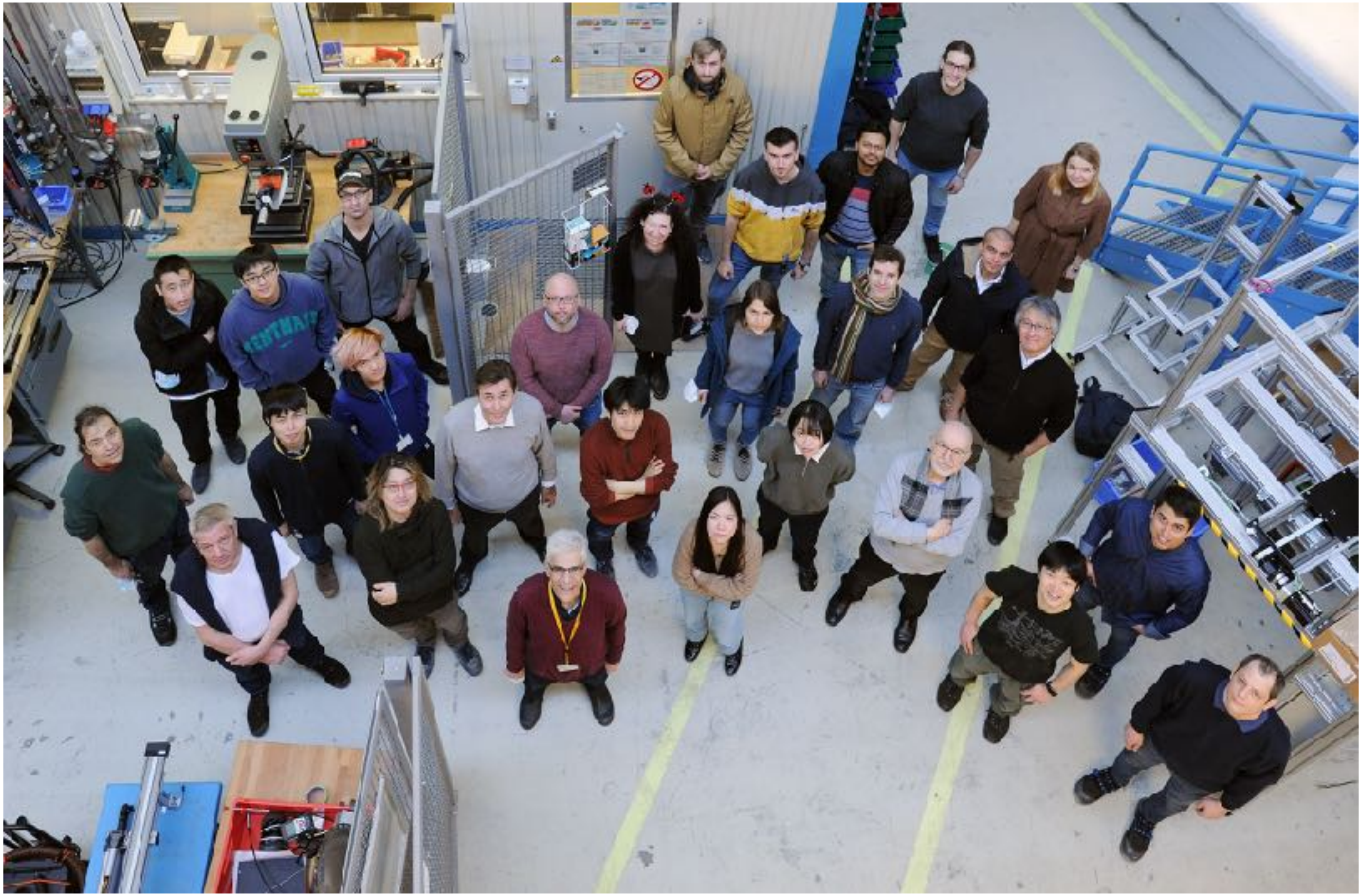

WASA-FRS / Super-FRS Experiment collaboration

WASA-FRS Experimental Setup

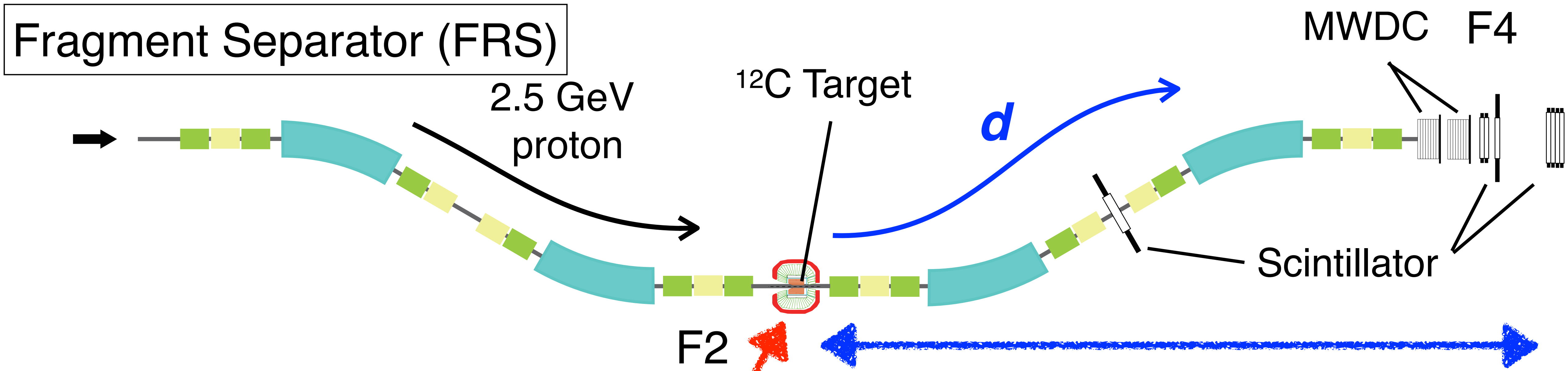

WASA for decay particle measurement

FRS (F2–F4) forward high-resolution spectroscopy

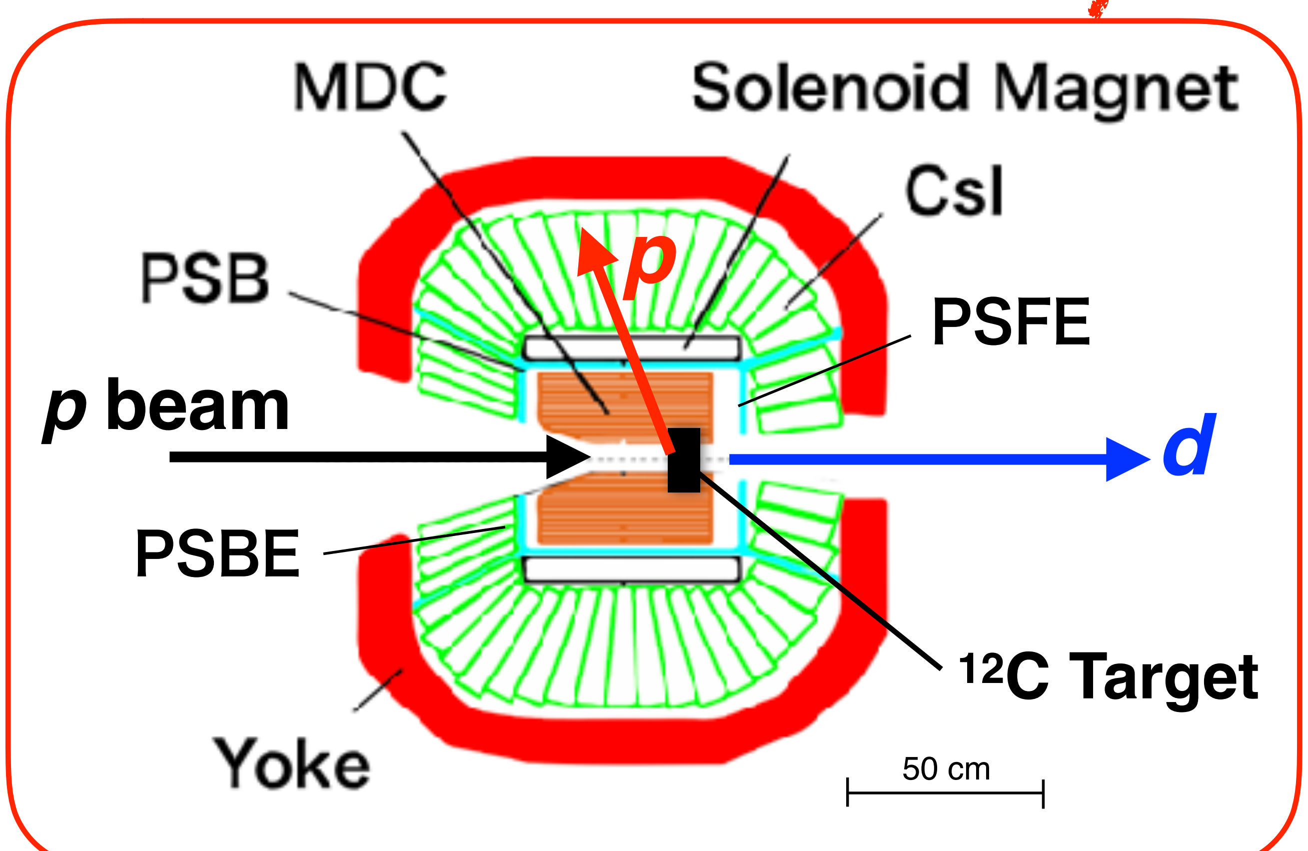

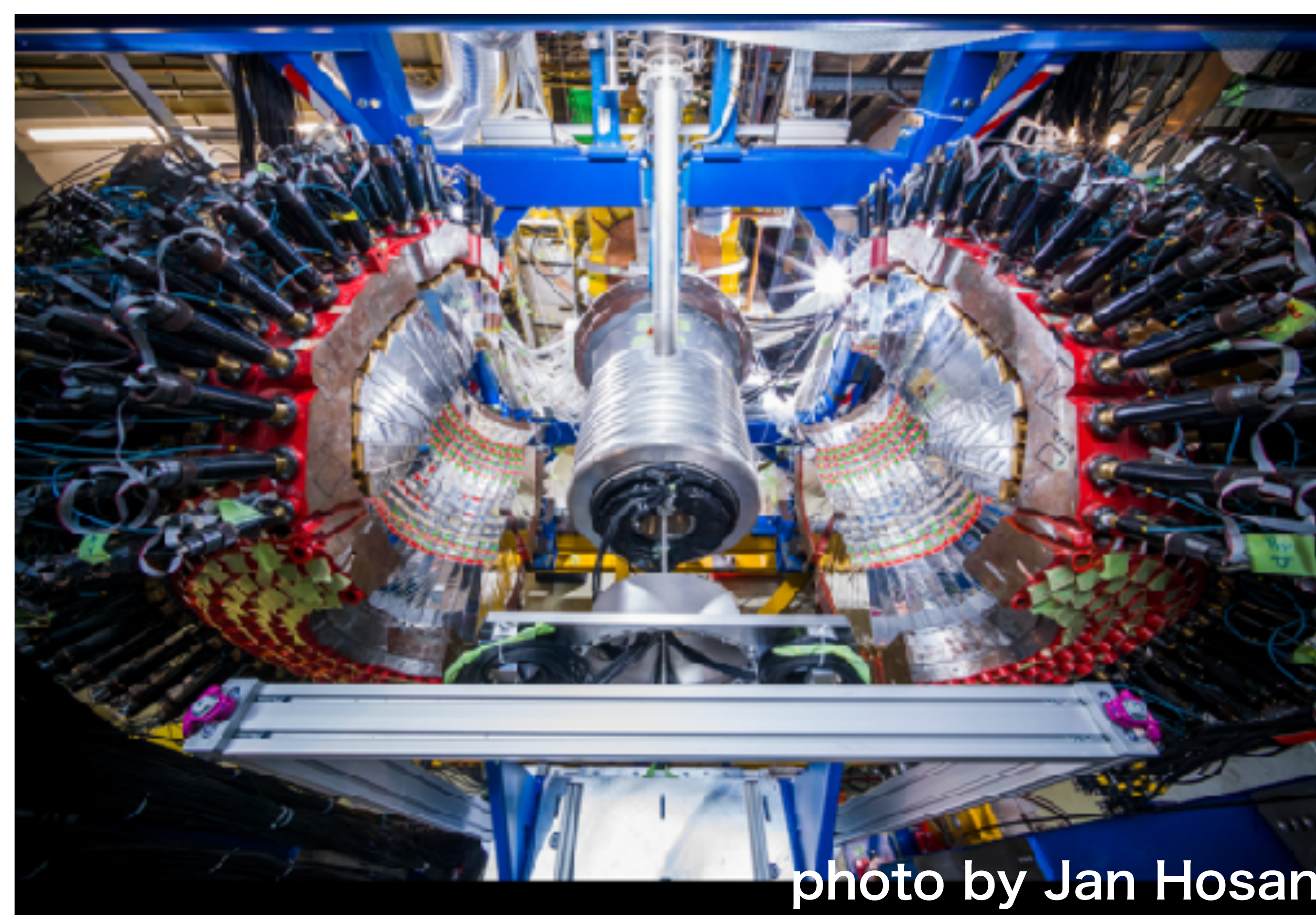

WASA-FRS Experimental Setup

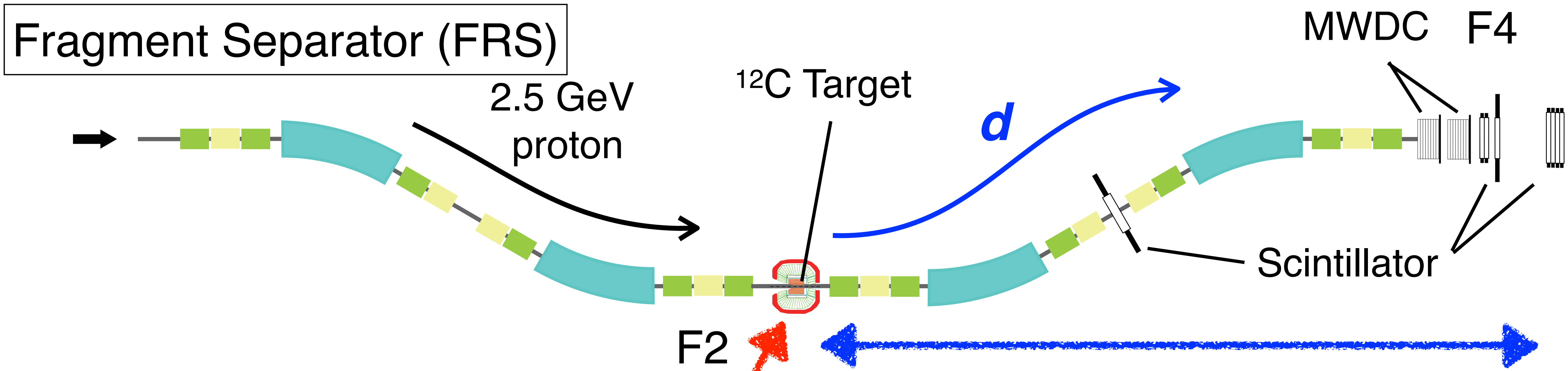

FRS (F2–F4) forward high-resolution spectroscopy

WASA for decay particle measurement

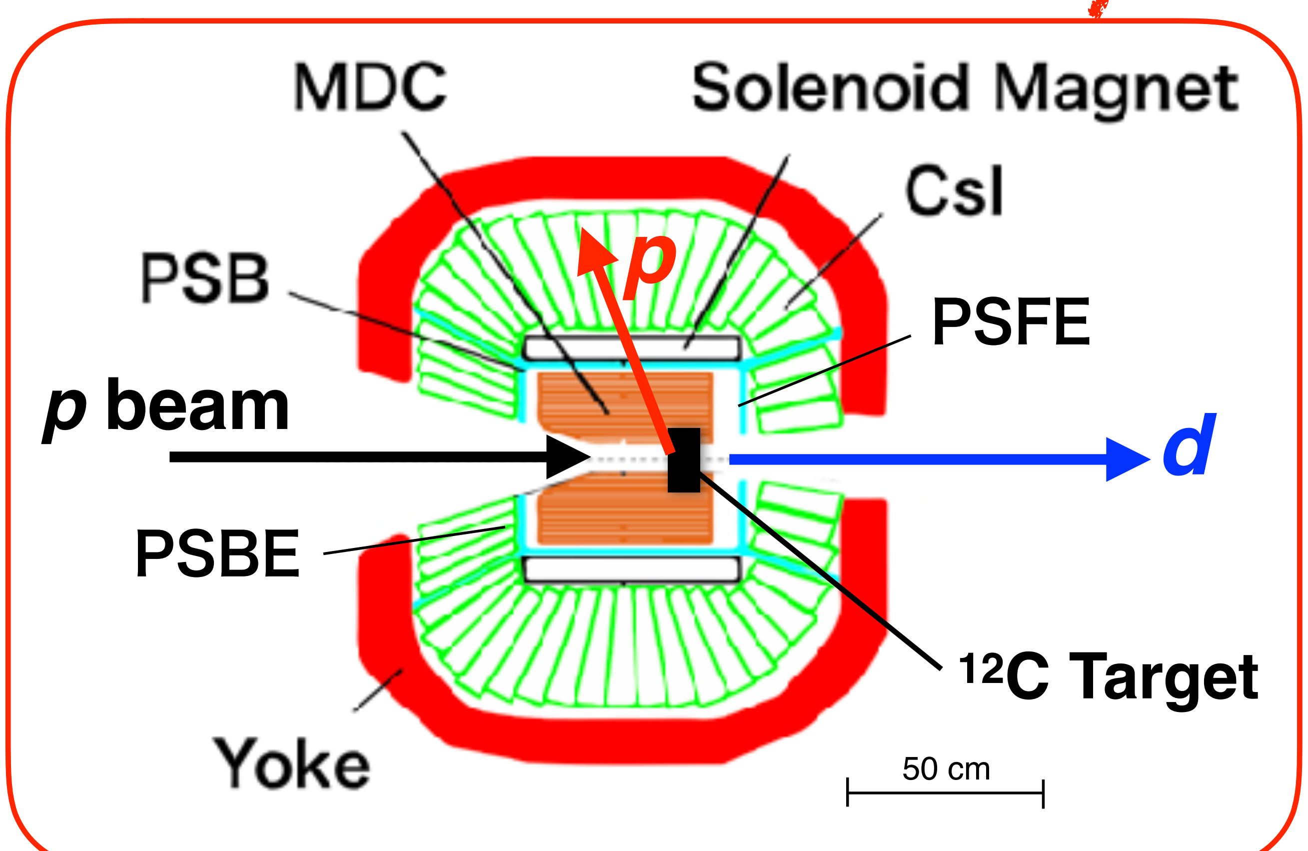

$$p + {}^{12}\mathrm{C} \rightarrow \underline{{}^{11}\mathrm{C}\times\eta'} + d$$
$$\hookrightarrow p + X$$

Analysis Status (FRS)

Forward Deuteron Analysis by FRS

- Deuteron identification
  with TOF selection

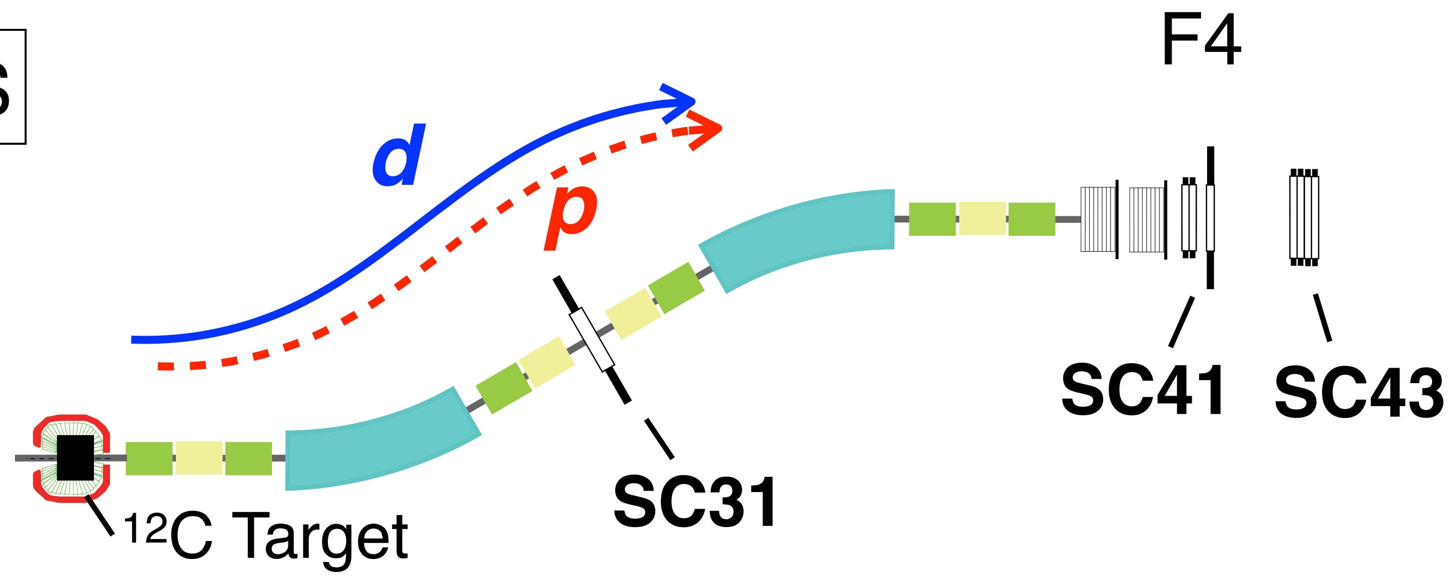

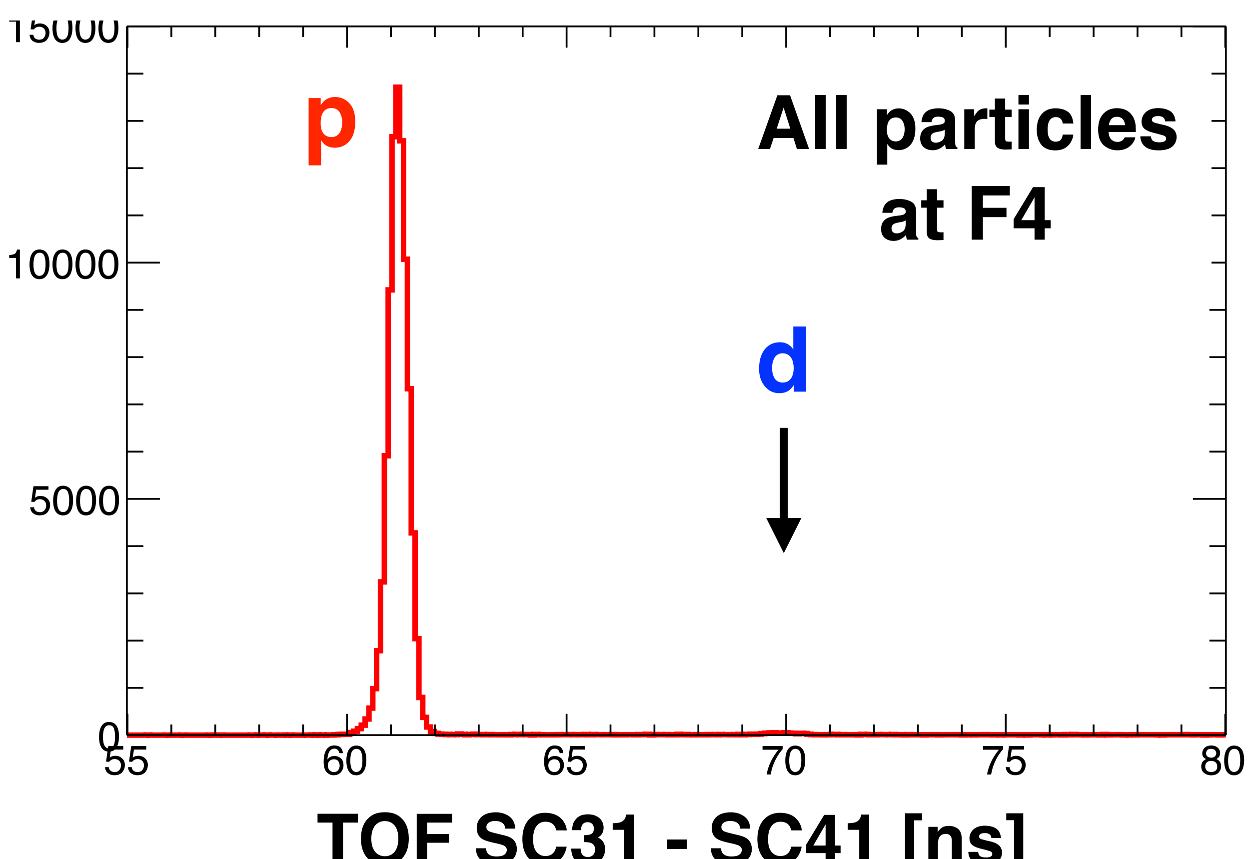

R. Sekiya, et al., presentation in Hadron2023, Y. K. Tanaka et al., Acta Phys. Pol. B Proc. Suppl.16, 4-A27 (2023)

Analysis Status (FRS)

Forward Deuteron Analysis by FRS

- Deuteron identification with TOF selection

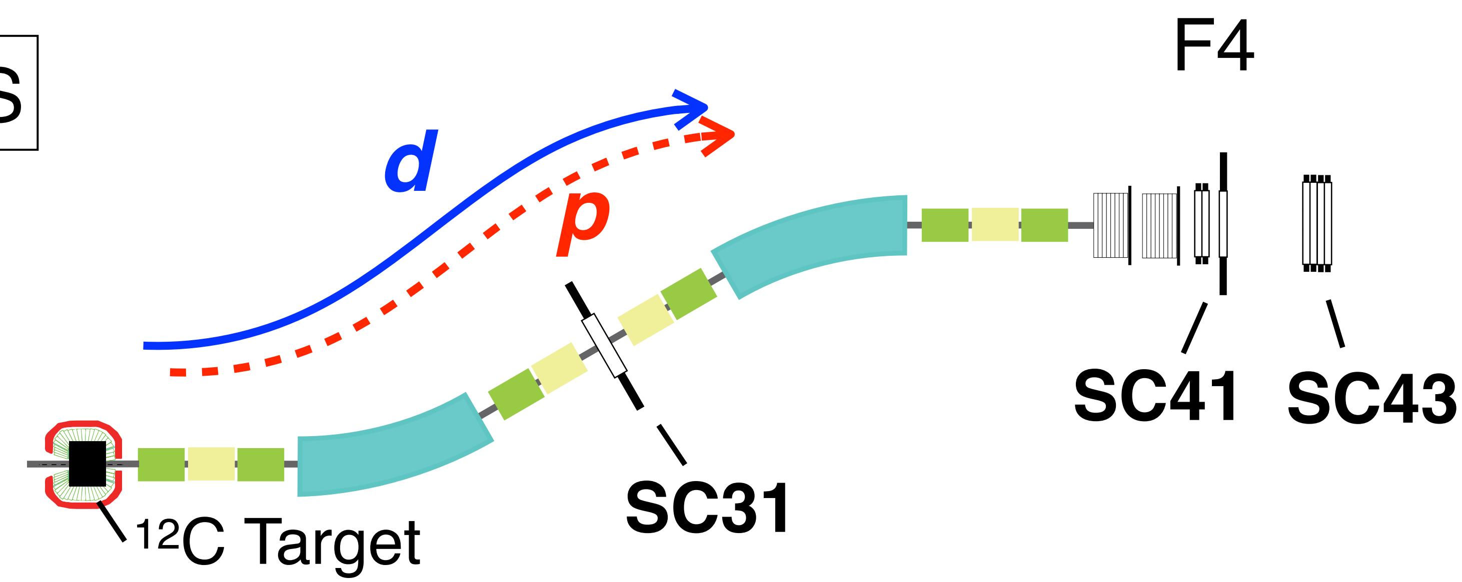

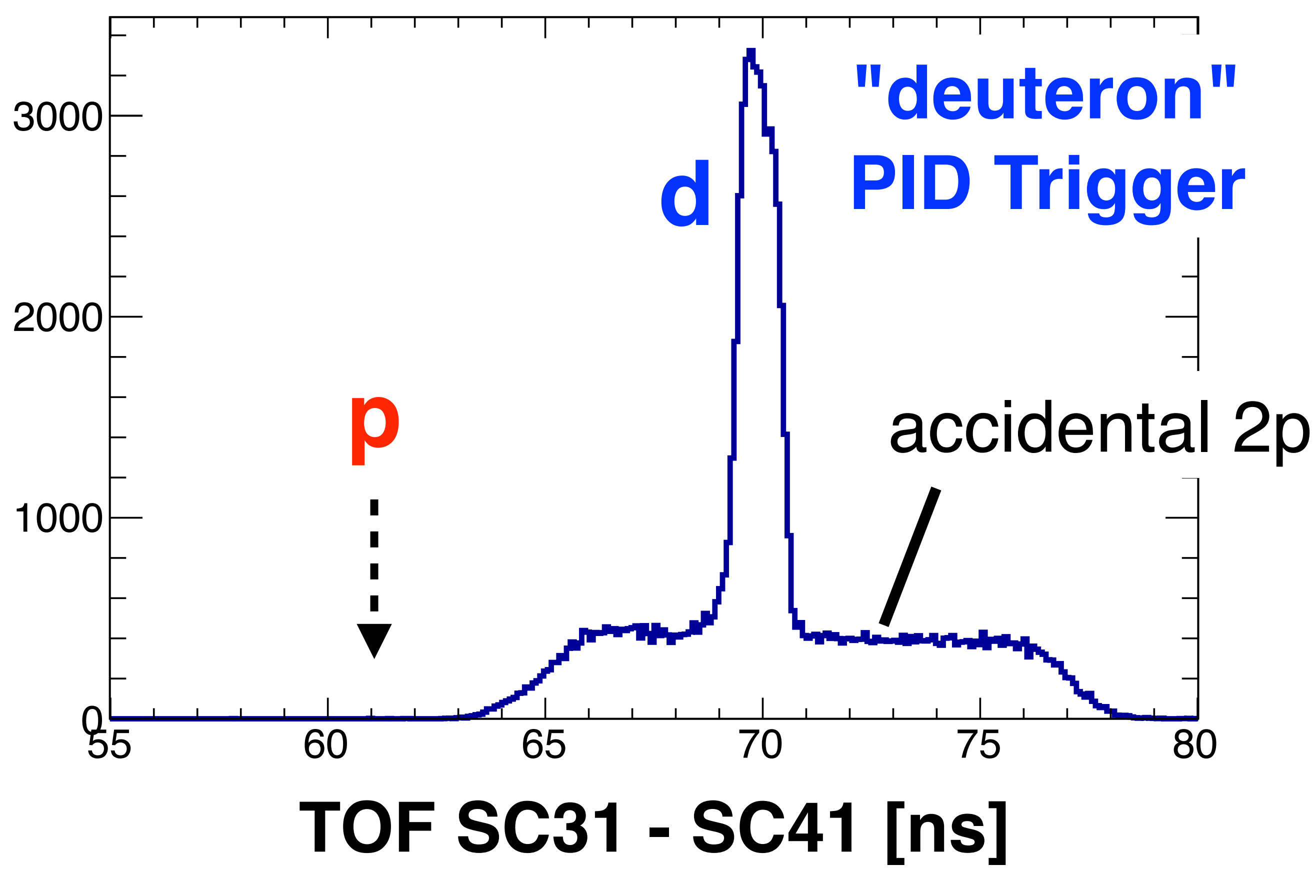

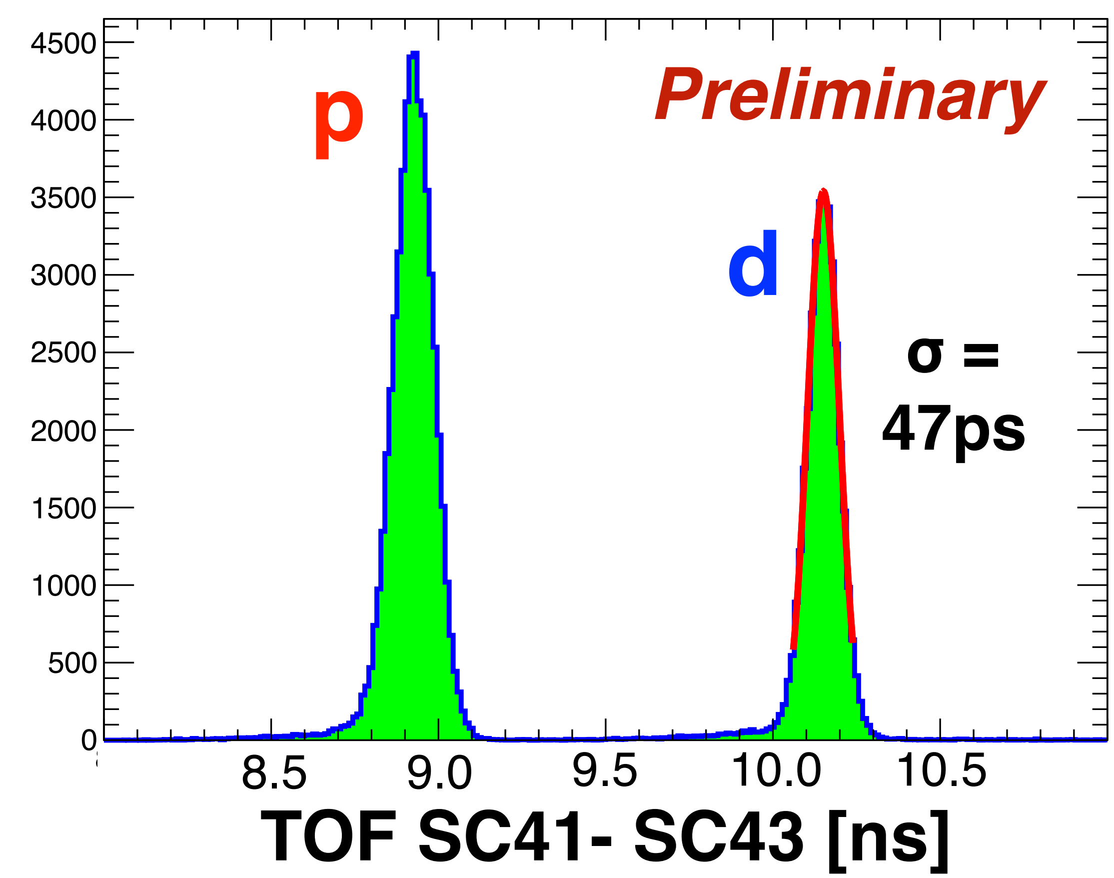

R. Sekiya, et al., presentation in Hadron2023, Y. K. Tanaka et al., Acta Phys. Pol. B Proc. Suppl.16, 4-A27 (2023)

Analysis Status (FRS)

Forward Deuteron Analysis by FRS

- Deuteron identification with TOF selection
- Missing-mass spectrum of $^{12}C(p,d)$ reaction (inclusive)

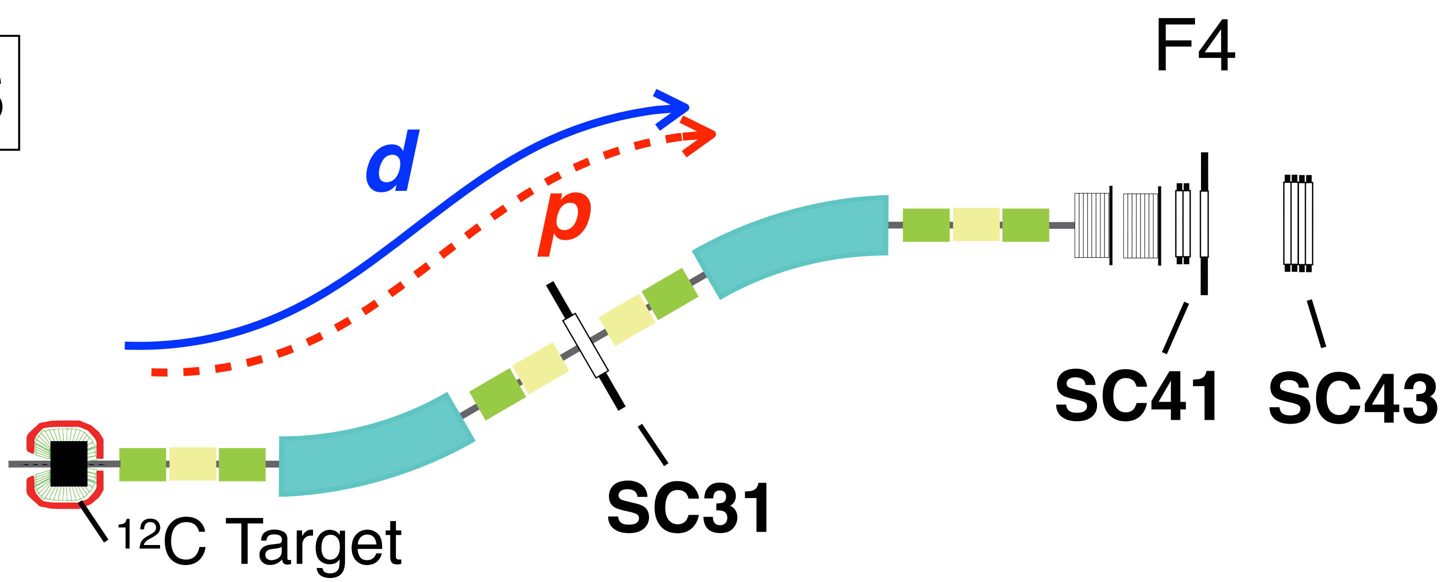

Analysis Status (WASA)

Decay Particle Analysis by WASA

- Plastic Scintillator ΔE and Timing
- Mini Drift Chamber tracking for momentum analysis
- CsI ΔE analysis

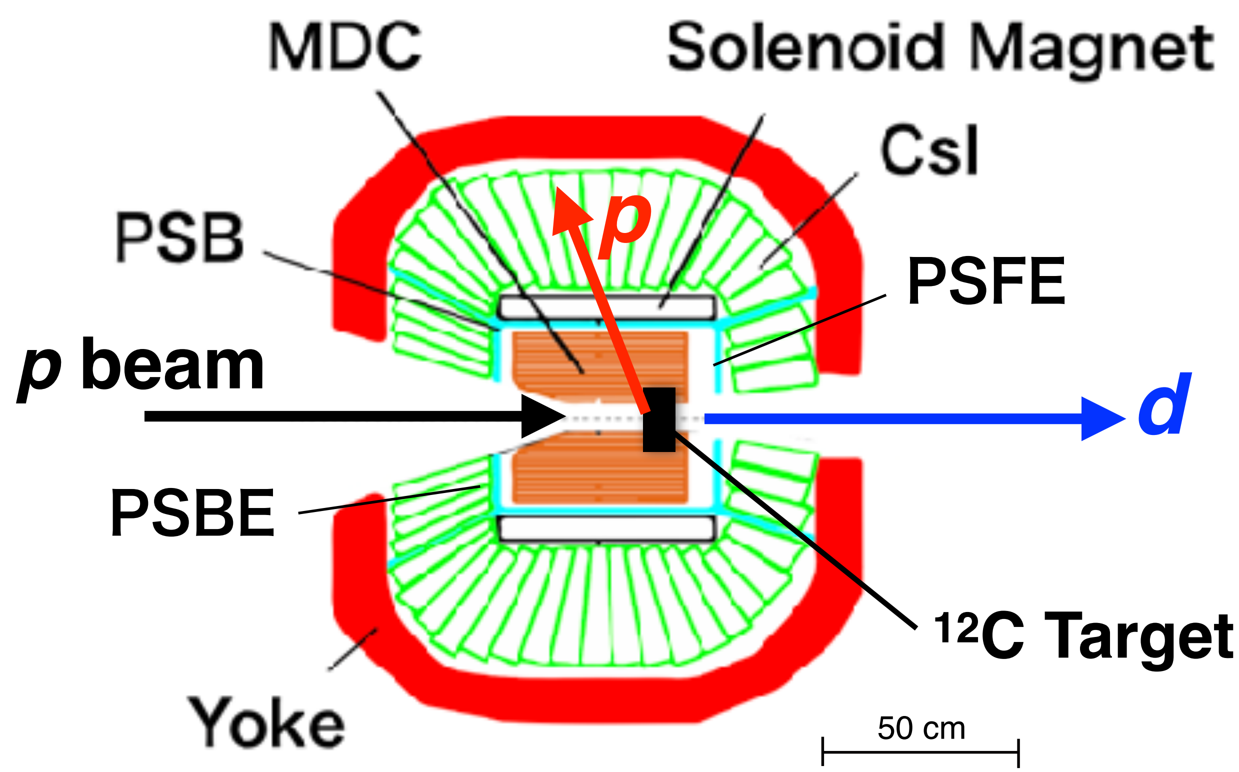

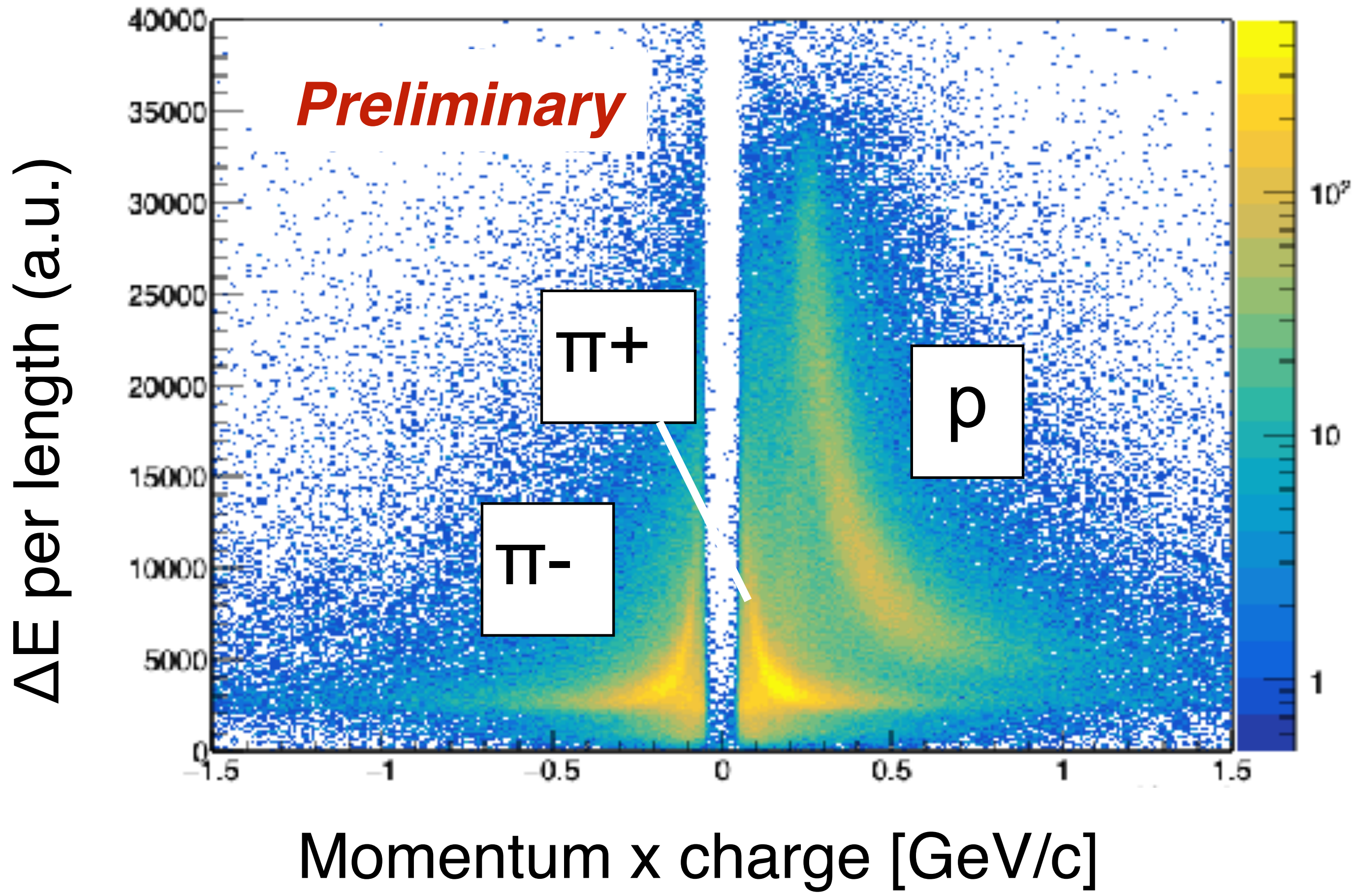

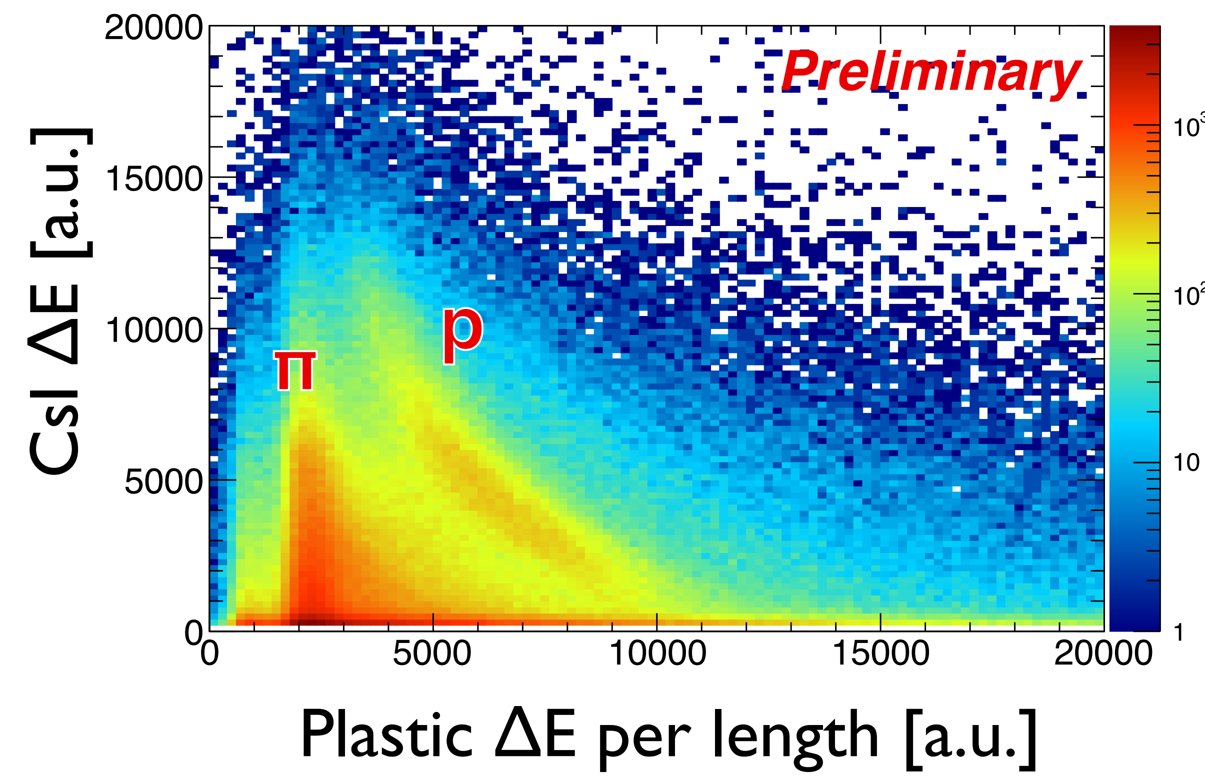

R. Sekiya, et al., presentation in Hadron2023, Y. K. Tanaka et al., Acta Phys. Pol. B Proc. Suppl.16, 4-A27 (2023)

Analysis Status (WASA)

Decay Particle Analysis by WASA

- Plastic Scintillator ΔE and Timing
- Mini Drift Chamber tracking for momentum analysis
- CsI ΔE analysis

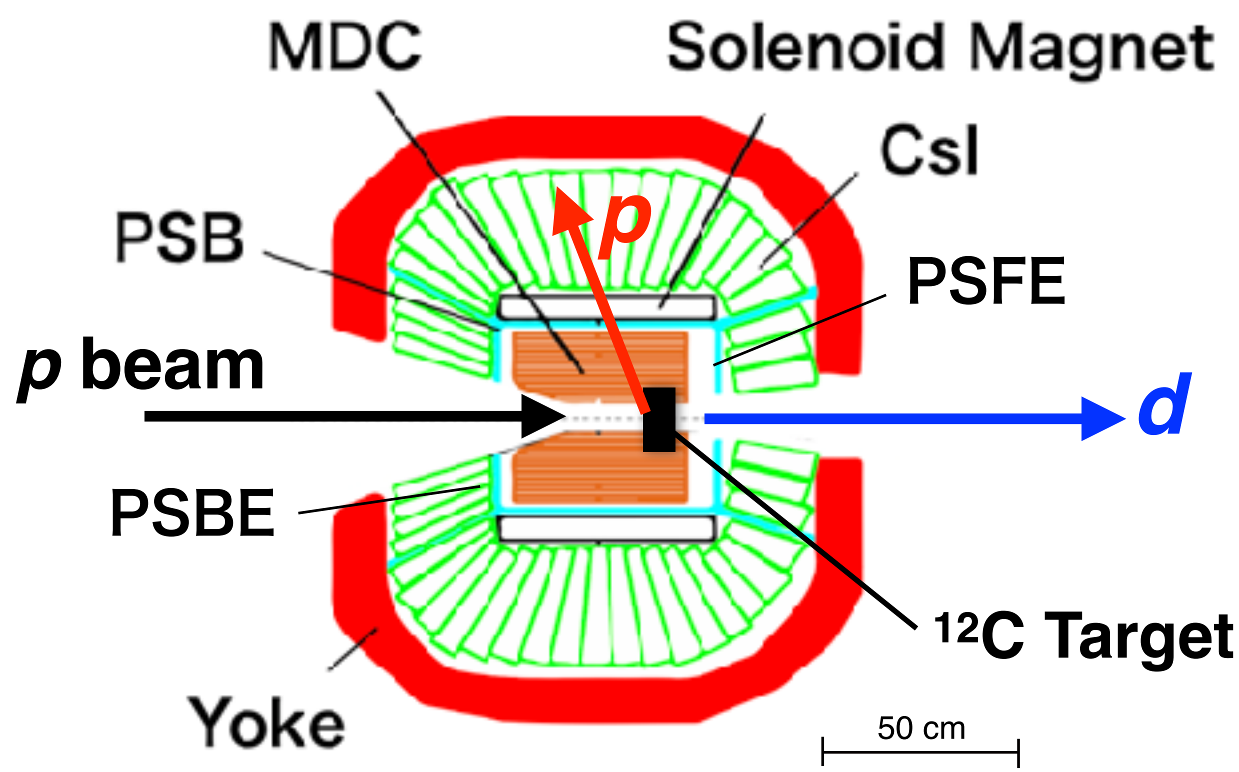

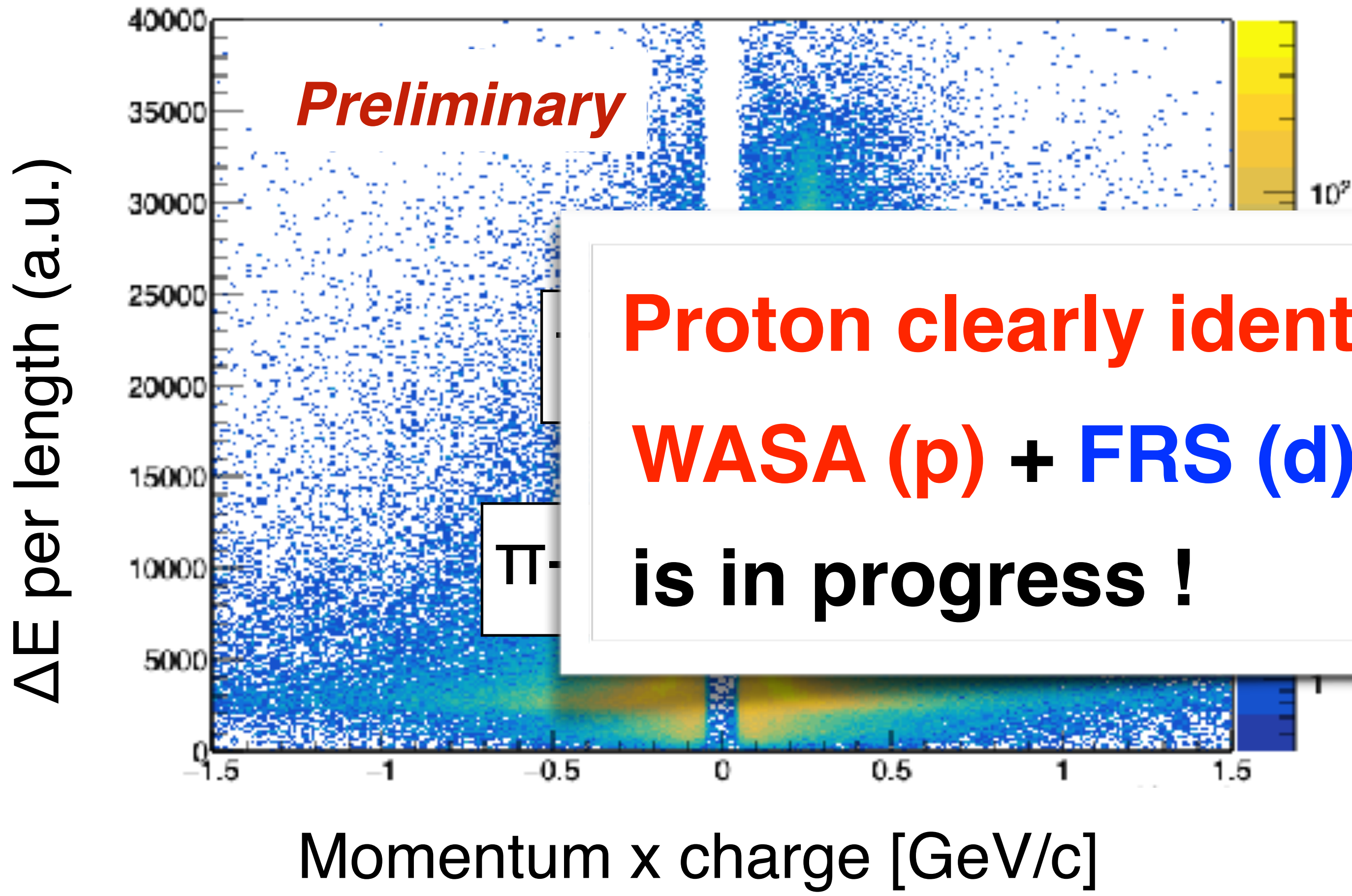

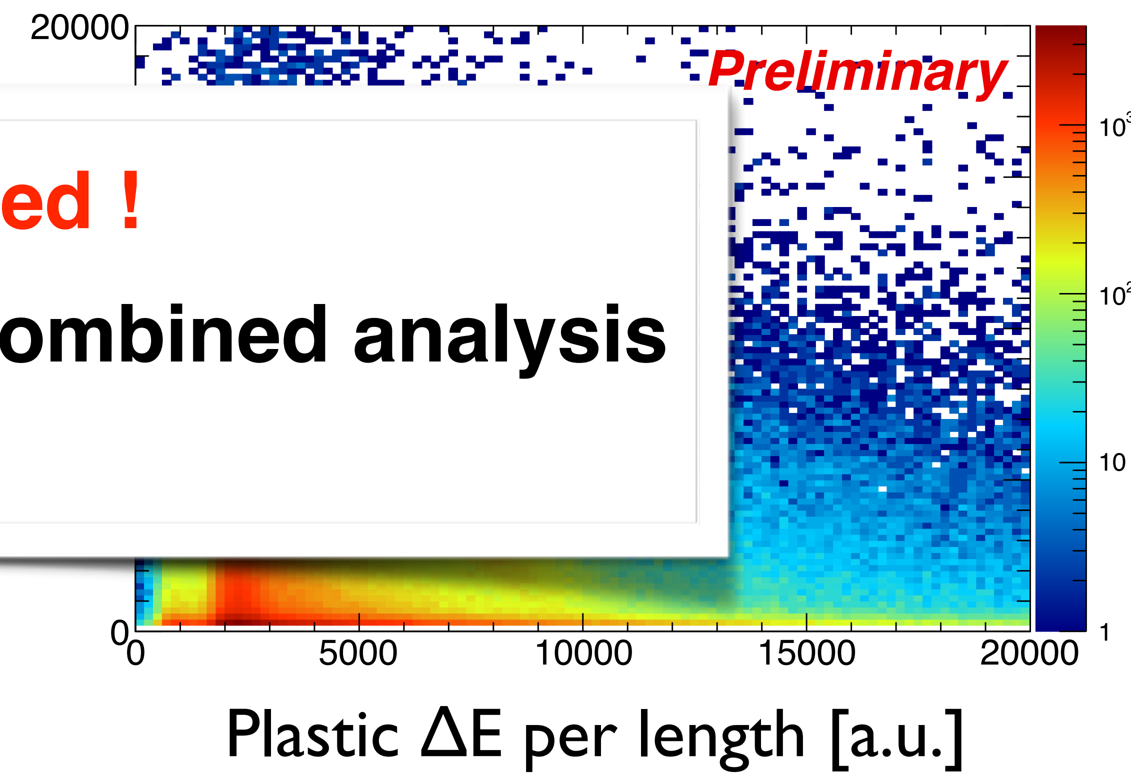

Proton clearly identified !

WASA (p) + FRS (d) combined analysis is in progress !

R. Sekiya, et al., presentation in Hadron2023, Y. K. Tanaka et al., Acta Phys. Pol. B Proc. Suppl.16, 4-A27 (2023)

Summary

- Meson-nucleus bound states are well-defined quantum states with finite overlap between meson and a nucleus and therefore provide possibilities to study QCD phenomena in finite nuclear density.

- Spectroscopy of deeply-bound π-atoms have contributed to experimental evaluation of partial restoration of chiral symmetry in finite nuclear density.
  - A recent high-precision experiment evaluated 23 ± 2 % reduction of chiral condensate at density $\rho_e = 0.58\ \rho_0$ (ρ_0 : normal nuclear density)
  - Further investigation of its ρ-dependence is ongoing by high-precision and systematic spectroscopy of pionic atoms with a wide range of nuclei.

- Experimental studies on η'-mesic nuclei are in progress to investigate in-medium η' properties in relation to $U_A(1)$ anomaly and chiral symmetry breaking.
  - First experiments did not observe bound states and evaluated upper limits on the formation cross section as well as on η'-nucleus potential parameters.
  - A new semi-exclusive experiment to search for η'-mesic nuclei with improved sensitivity has been performed in 2022 with the WASA-FRS setup at GSI/FAIR. Data analysis is in progress.